Theory of electron- and neutrino-nucleus scattering

Noemi Rocco

NUFACT, 'The 20th International Workshop on Neutrinos from Accelerator'
August 12-18, 2018

In Collaboration with:

C. Barbieri (University of Surrey), O. Benhar (La Sapienza), A. Lovato (Argonne National Laboratory), V. Somà (Cea-Irfu)

Outline

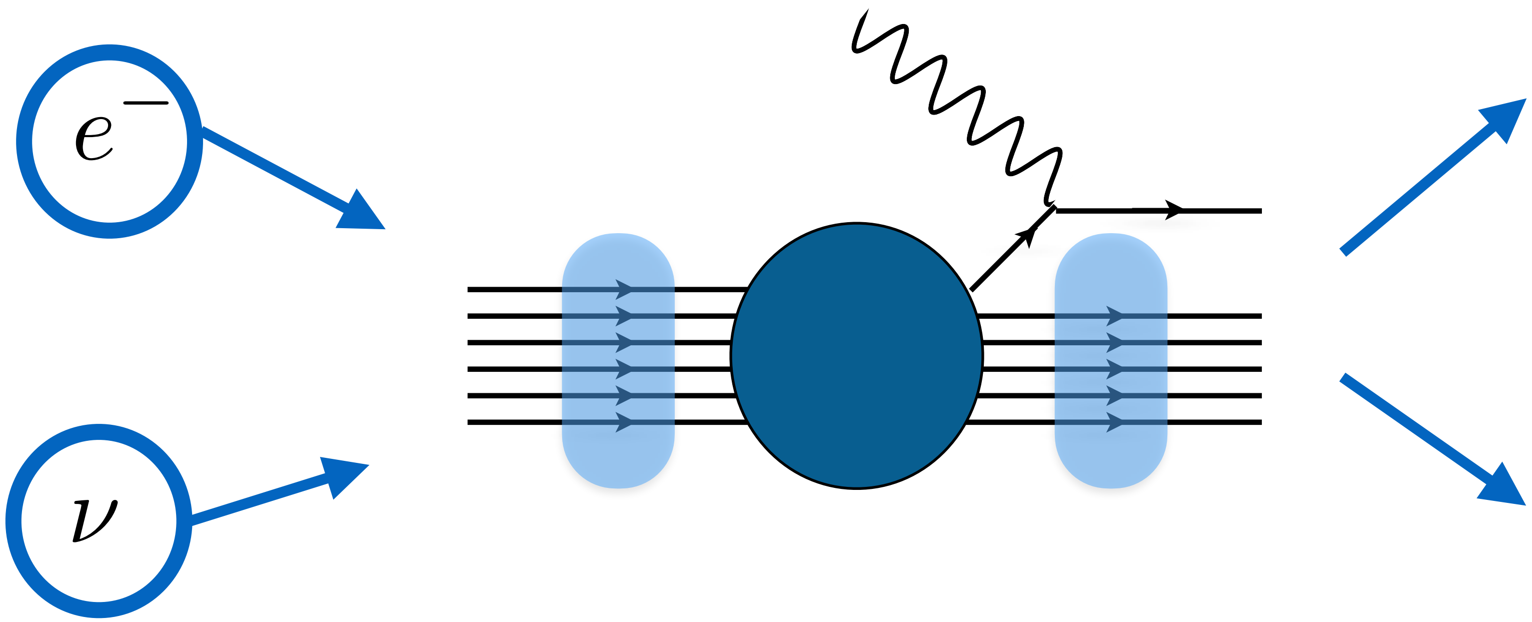

Self Consistent Green's Function

Correlated Basis Function

Electron-nucleus scattering

Schematic representation of the inclusive cross section as a function of the energy loss.

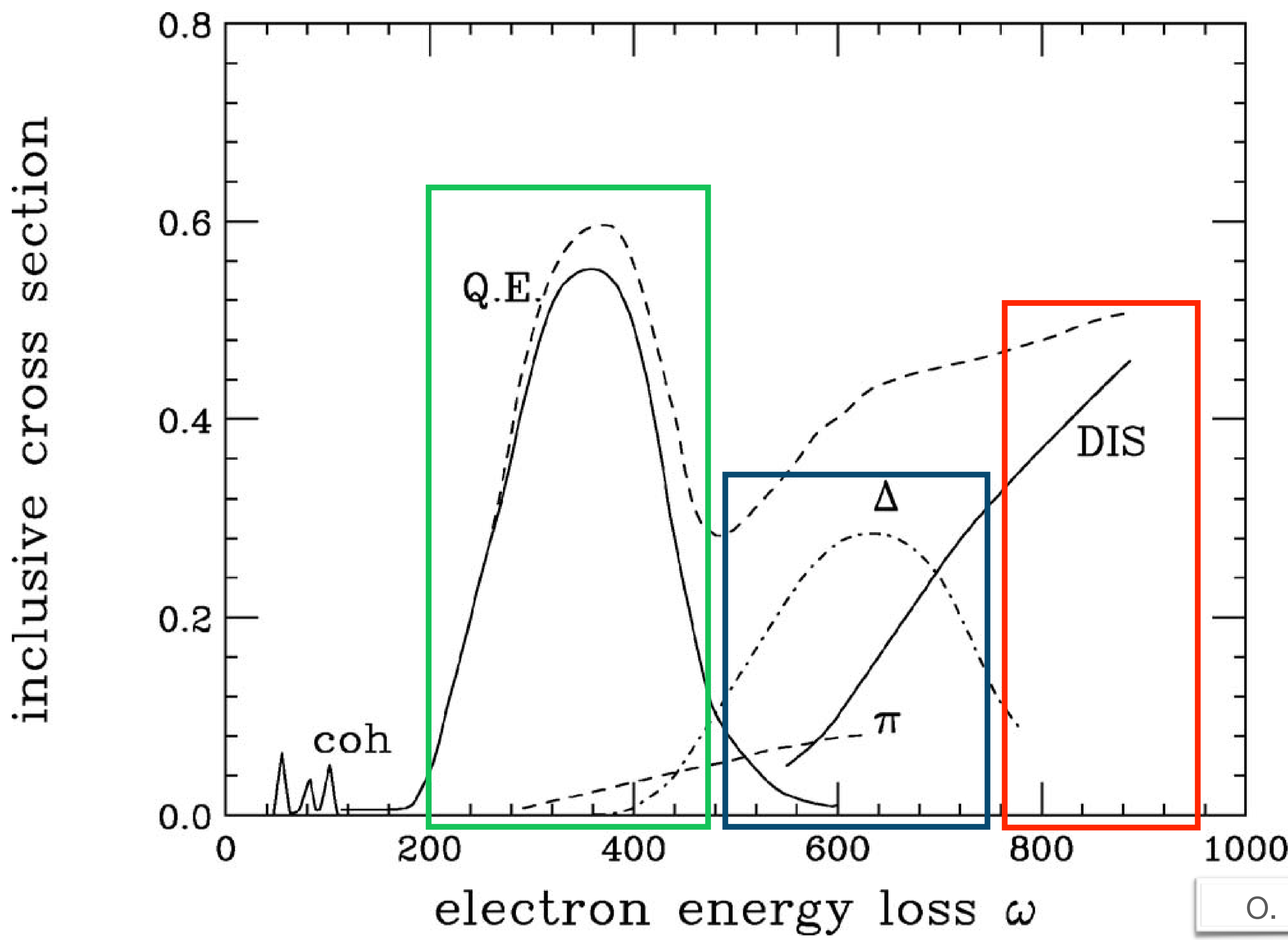

- Broad peak due to quasi-elastic electron-nucleon scattering.
- Excitation of the nucleon to distinct resonances (like the Δ) and pion production.
- Deep Inelastic Scattering region, productions of hadrons other than protons and neutrons

O. Benhar, et al. RMP **80**, 189 (2008)

The different reaction mechanisms can be easily identified

Neutrinos' challenge

In neutrino-oscillation experiments the use of nuclear target as detectors allows for a substantial increase of the event rate: Nuclear Theory comes into play

What are the goals to be achieved by theory?

- Understanding neutrino-nucleus interactions in the 1-10 GeV spectrum
- Accurate description of both nuclear dynamics and of the interaction vertex where relativistic effects are accounted for
- Develop an approach able to tackle all the different reaction mechanisms in a consistent way
- Describe medium mass nuclei (^{12}C, ^{16}O) + large mass, isospin asymmetric, open shell nuclei (^{40}Ar)

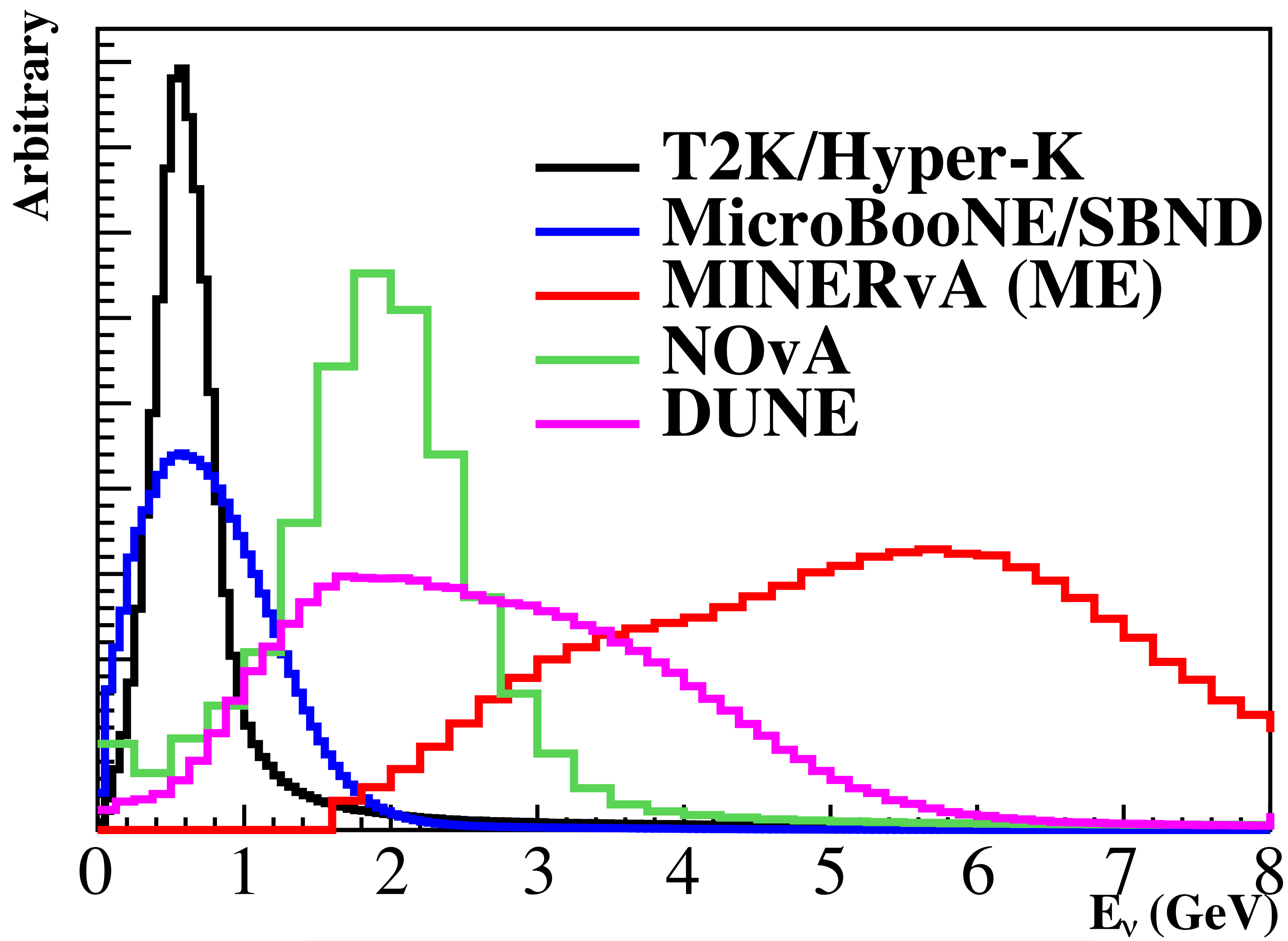

T. Katori and M. Martini,. arXiv:1611.07770

Electron-nucleus scattering

The inclusive cross section of the process in which a lepton scatters off a nucleus and the hadronic final state is undetected can be written as

$$\frac{d^2\sigma}{d\Omega_\ell dE_{\ell'}} = L_{\mu\nu} W^{\mu\nu}$$

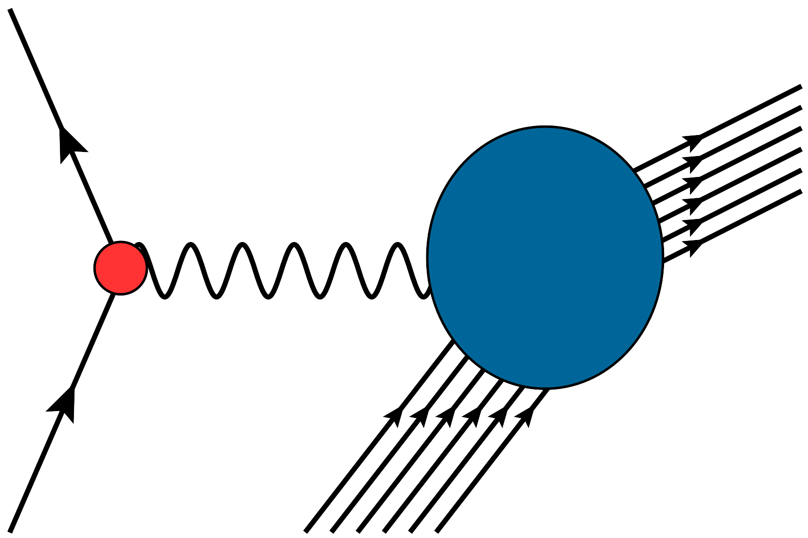

- The Leptonic tensor is fully specified by the lepton kinematic variables. For instance, in the electron-nucleus scattering case

$$L^{\rm EM}_{\mu\nu} = 2[k_\mu k'_\nu + k_\nu k'_\mu - g_{\mu\nu}(kk')]$$

- The Hadronic tensor contains all the information on target response

$$W^{\mu\nu} = \sum_f \langle 0|J^{\mu\,\dagger}(q)|f\rangle\langle f|J^\nu(q)|0\rangle\delta^{(4)}(p_0 + q - p_f)$$

Non relativistic nuclear many-body theory (NMBT) provides a fully consistent theoretical approach allowing for an accurate description of |0>, independent of momentum transfer.

The Impulse Approximation

- For sufficiently large values of $|\mathbf{q}|$, the IA can be applied under the assumptions

$$|f\rangle \longrightarrow |p\rangle \otimes |f\rangle_{A-1} \qquad J_\alpha = \sum_i j^i_\alpha$$

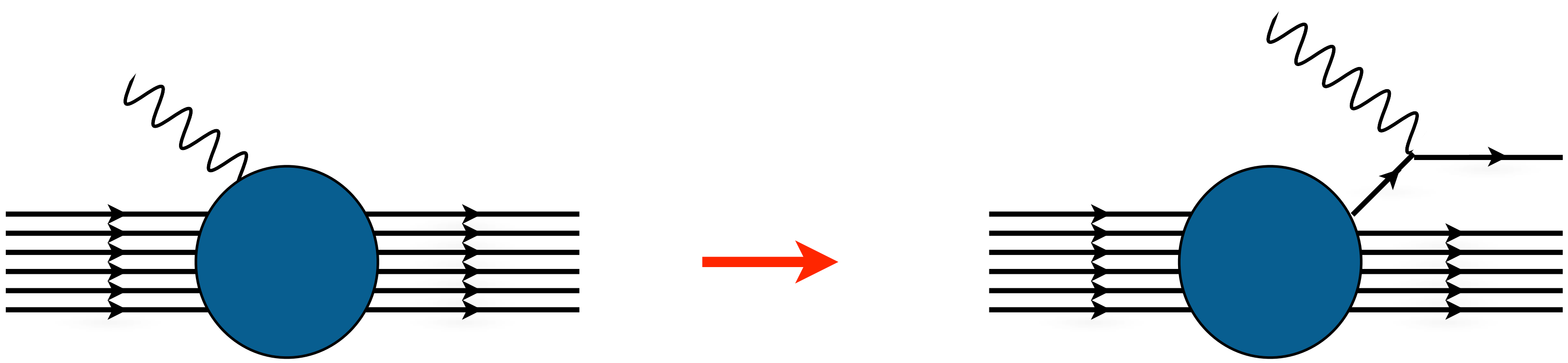

- The matrix element of the current can be written in the factorized form

$$\langle 0|J_\alpha|f\rangle \to \sum_k \langle 0|[|k\rangle \otimes |f\rangle_{A-1}]\langle k|\sum_i j^i_\alpha|p\rangle$$

- The nuclear cross section is given in terms of the one describing the interaction with individual bound nucleons

$$d\sigma_A = \int dE\, d^3k\, d\sigma_N P(\mathbf{k}, E)$$

- The intrinsic properties of the nucleus are described by the hole spectral function

The one-body hole Spectral Function

- The nuclear matrix element can be rewritten in terms of the transition amplitude

$$[\langle\psi_f^{A-1}|\otimes\langle k|]|\psi_0^A\rangle=\sum_\alpha \mathcal{Y}_{f,\alpha}\tilde{\Phi}_\alpha(\mathbf{k})=\sum_\alpha \tilde{\Phi}_\alpha(\mathbf{k})\langle\psi_f^{A-1}|a_\alpha|\psi_0^A\rangle\,,$$

- The Spectral Function gives the probability distribution of removing a nucleon with momentum **k**, leaving the spectator system with an excitation energy E

$$P_h(\mathbf{k},E)=\sum_f|\langle\psi_0^A|[|\mathbf{k}\rangle\otimes|\psi_f^{A-1}\rangle]|^2\delta(E+E_f^{A-1}-E_0^A)$$

$$=\frac{1}{\pi}\sum_{\alpha\beta}\tilde{\Phi}^*_\beta(\mathbf{k})\tilde{\Phi}_\alpha(\mathbf{k})\mathrm{Im}\langle\psi_0^A|a_\beta^\dagger\frac{1}{E+(H-E_0^A)-i\epsilon}a_\alpha|\psi_0^A\rangle\,.$$

- The two points Green's Function describes nucleon propagation in the nuclear medium

$$G_{h,\alpha\beta}(E)=\langle\psi_0^A|a_\beta^\dagger\frac{1}{E+(H-E_0^A)-i\epsilon}a_\alpha|\psi_0^A\rangle$$

Self Consistent Green's Function

- The one-body Green's function is completely determined by solving the Dyson equation

$$G_{\alpha\beta}(E) = G^0_{\alpha\beta}(E) + \sum_{\gamma\delta} G^0_{\alpha\gamma}\Sigma^*_{\gamma\delta}(E) G_{\delta\beta}(E)$$

$G^0_{\alpha\beta}(E)$ → initial reference state, HF

$\Sigma^*_{\gamma\delta}(E)$ → Self energy: encoding nuclear medium effects on the particle propagation

$G_{\delta\beta}(E)$ → Correlated propagator

- $\Sigma^* = \Sigma^*[G(E)]$, an iterative procedure is required to solve the Dyson equation self-consistently

- The self-energy is systematically calculated in a non-perturbative fashion within the Algebraic Diagrammatic Construction (ADC). The saturating chiral interaction at NNLO ($NNLO_{sat}$) is used.

✤ V. Somà et al, Phys.Rev. C87 (2013) no.1, 011303 : generalization of this formalism within Gorkov theory allows to describe open-shell nuclei such as Ar^{40}, Ti^{48} …

- How can we test this ab initio approach? Static nuclear observables can be used to check the goodness (understand the limitations) of the model

Benchmark the nuclear model: ^{16}O charge density distribution

- The nuclear charge density distribution is the Fourier transform of the charge elastic form factor:

$$\rho_{ch}(r') = \int \frac{d^3q}{(2\pi)^3} e^{-i\mathbf{q}\cdot\mathbf{r}'} \; F_L(\mathbf{q})$$

NR, C. Barbieri, Phys.Rev. C98 (2018) 025501

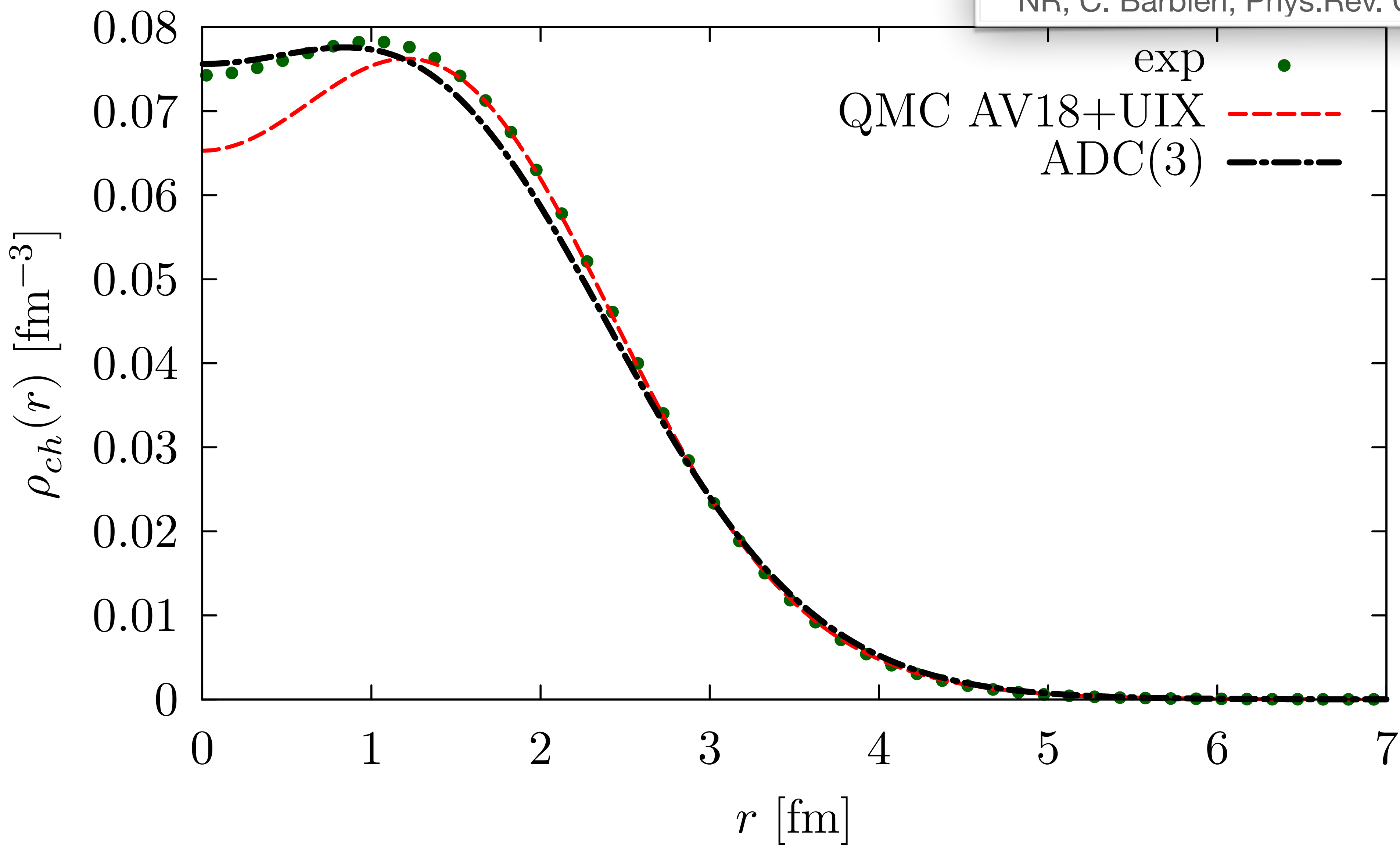

- Nice agreement between the SCGF and QMC calculations
- SCGF results agree with experiments (corroborates the goodness of NNLO$_{sat}$)

Benchmark the nuclear model: ^{16}O elastic form factor

- The charge elastic form factor is given by $$F_L(\mathbf{q}) = \frac{1}{Z}\frac{G_E^p(Q_{el}^2)\tilde{\rho}_p(q) + G_E^n(Q_{el}^2)\tilde{\rho}_n(q)}{\sqrt{1+Q_{el}^2/(4m^2)}},$$

NR, C. Barbieri, Phys.Rev. C98 (2018) 025501

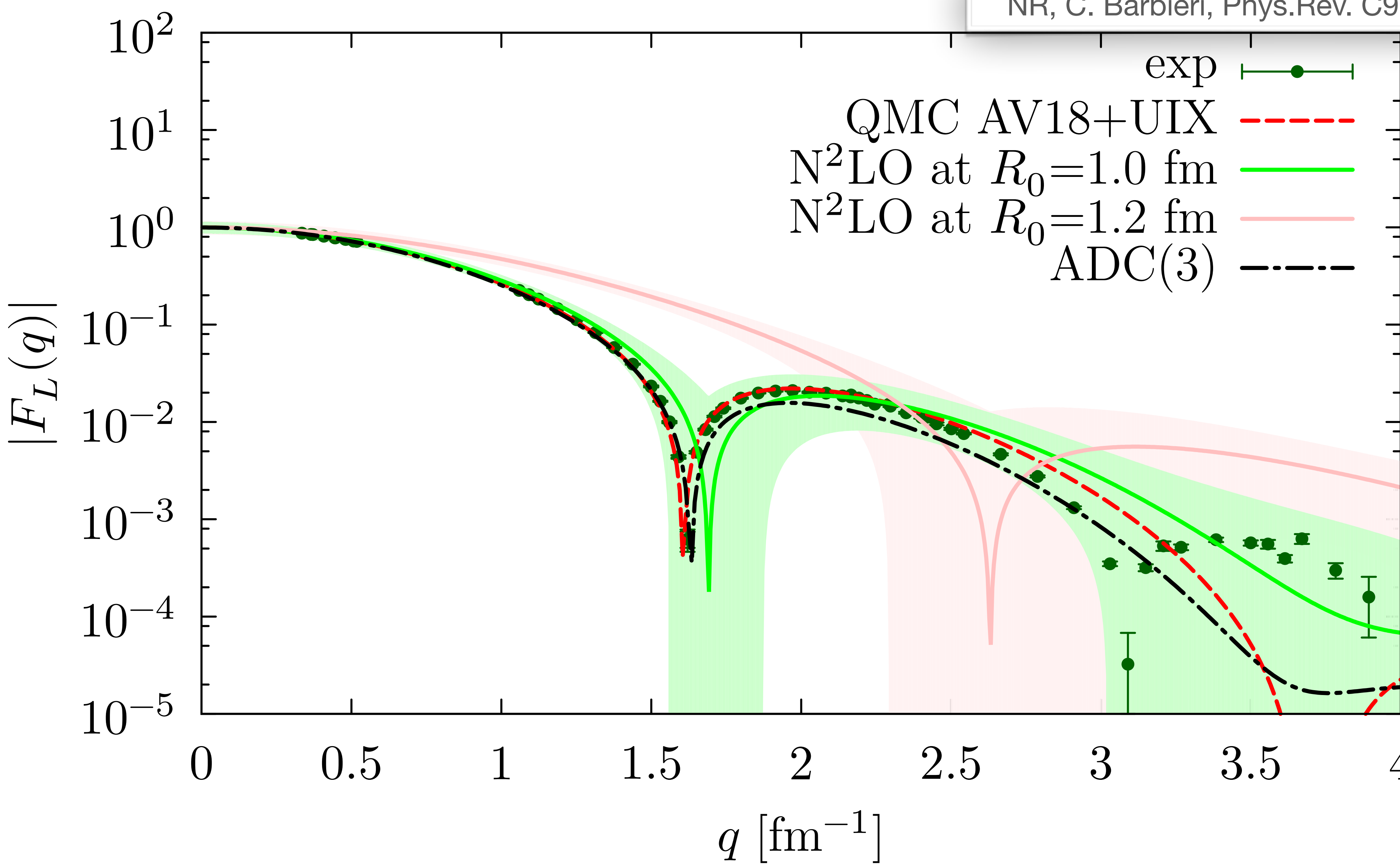

✤ The N^{2}LO results are taken from D. Lonardoni, et. al, Phys. Rev. C97, 044318 (2018) where two different coordinate-space cutoffs have been adopted

Benchmark the nuclear model: ^{16}O momentum distribution

- Single particle momentum distribution of ^{16}O

NR, C. Barbieri, Phys.Rev. C98 (2018) 025501

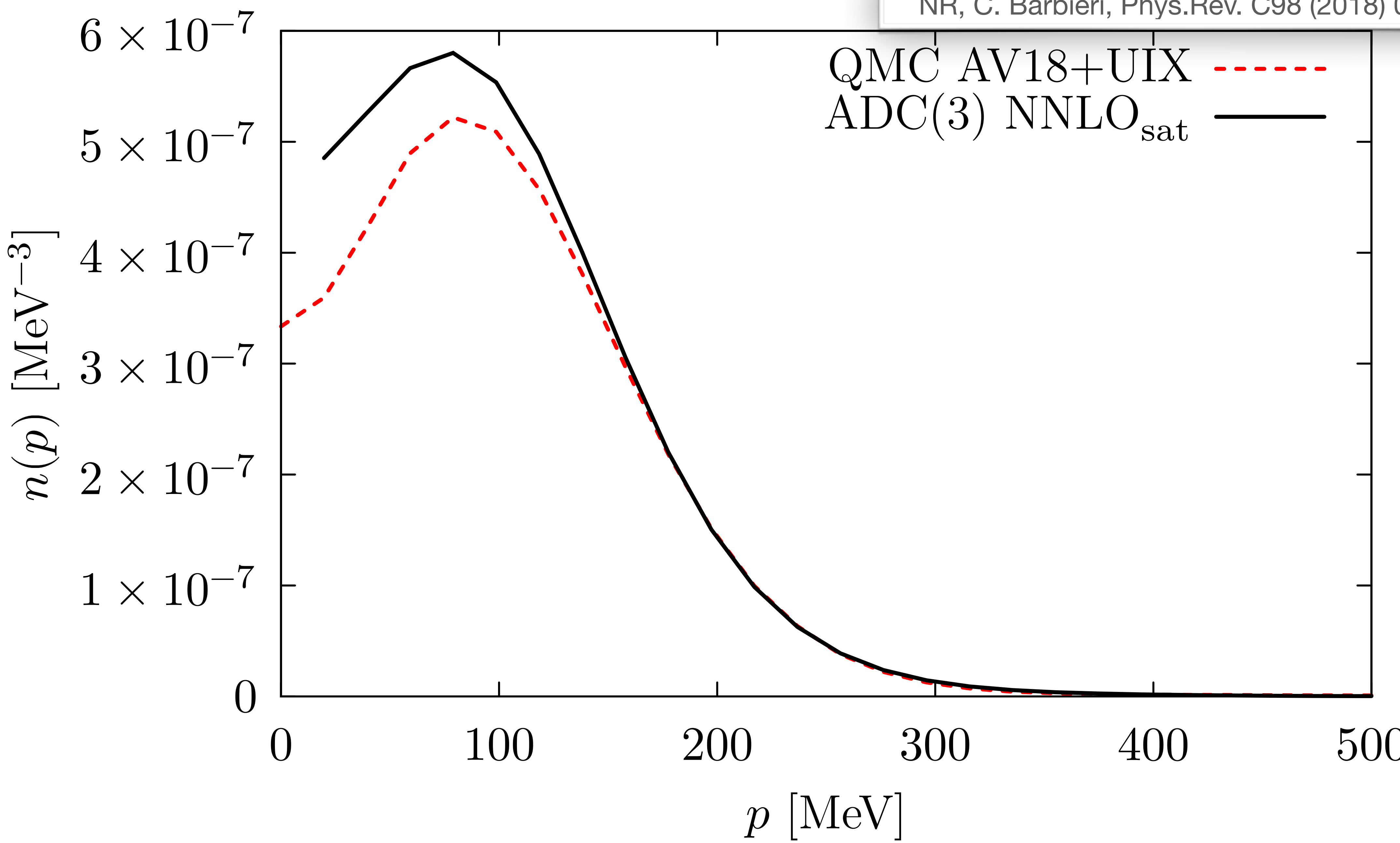

- The momentum distribution reflects the fact that NNLO$_{sat}$ is softer the AV18+UIX.

Benchmark the nuclear model: ^{16}O momentum distribution

- Single particle momentum distribution of ^{16}O, log scale

NR, C. Barbieri, Phys.Rev. C98 (2018) 025501

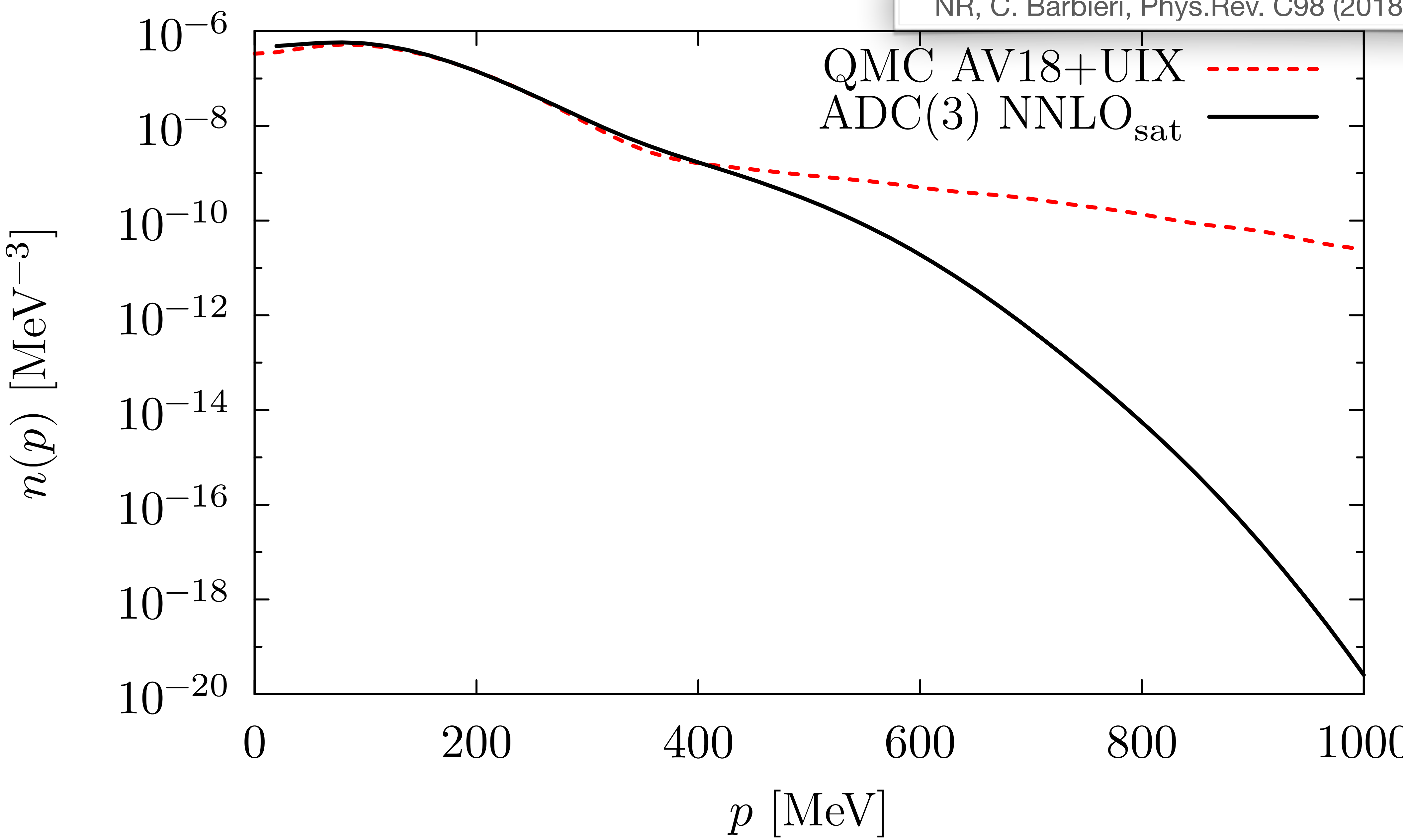

- The momentum distribution reflects the fact that NNLO$_{sat}$ is softer than AV18+UIX.

The Impulse Approximation and convolution scheme

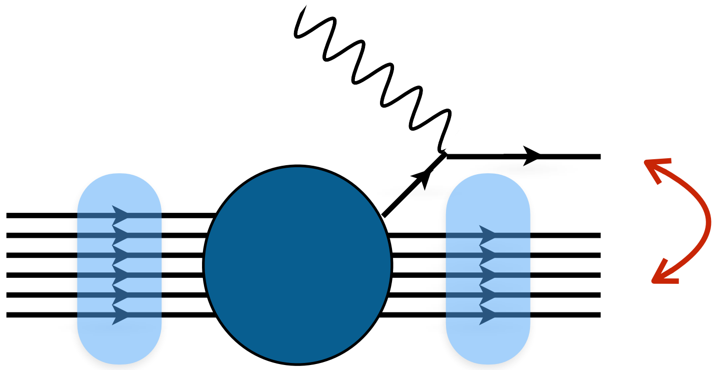

- In the kinematical region in which the interactions between the struck particle and the spectator system can not be neglected, the IA results have to be modified to include the effect of final state interactions (FSI).

$$d\sigma_{FSI} = \int d\omega' f_{\mathbf{q}}(\omega - \omega') d\tilde{\sigma}_{IA} \quad , \quad \tilde{e}(\mathbf{p}) = e(\mathbf{p}) + \mathcal{U}(t_{kin}(\mathbf{p}))$$

Optical Potential

- The theoretical approach to calculate the folding function consists on a generalization of Glauber theory of high energy proton-nucleus scattering

$$f_{\mathbf{q}}(\omega) = \delta(\omega)\sqrt{T_{\mathbf{q}}} + \int \frac{dt}{2\pi} e^{i\omega t} \left[\bar{U}_{\mathbf{q}}^{FSI}(t) - \sqrt{T_{\mathbf{q}}} \right]$$

Nuclear Transparency

Glauber Factor

A.Ankowski et al,Phys. Rev. D91, 033005 (2015)

O.Benhar, Phys. Rev. C87, 024606 (2013)

^{16}O(e,e') cross sections within the SCGF approach

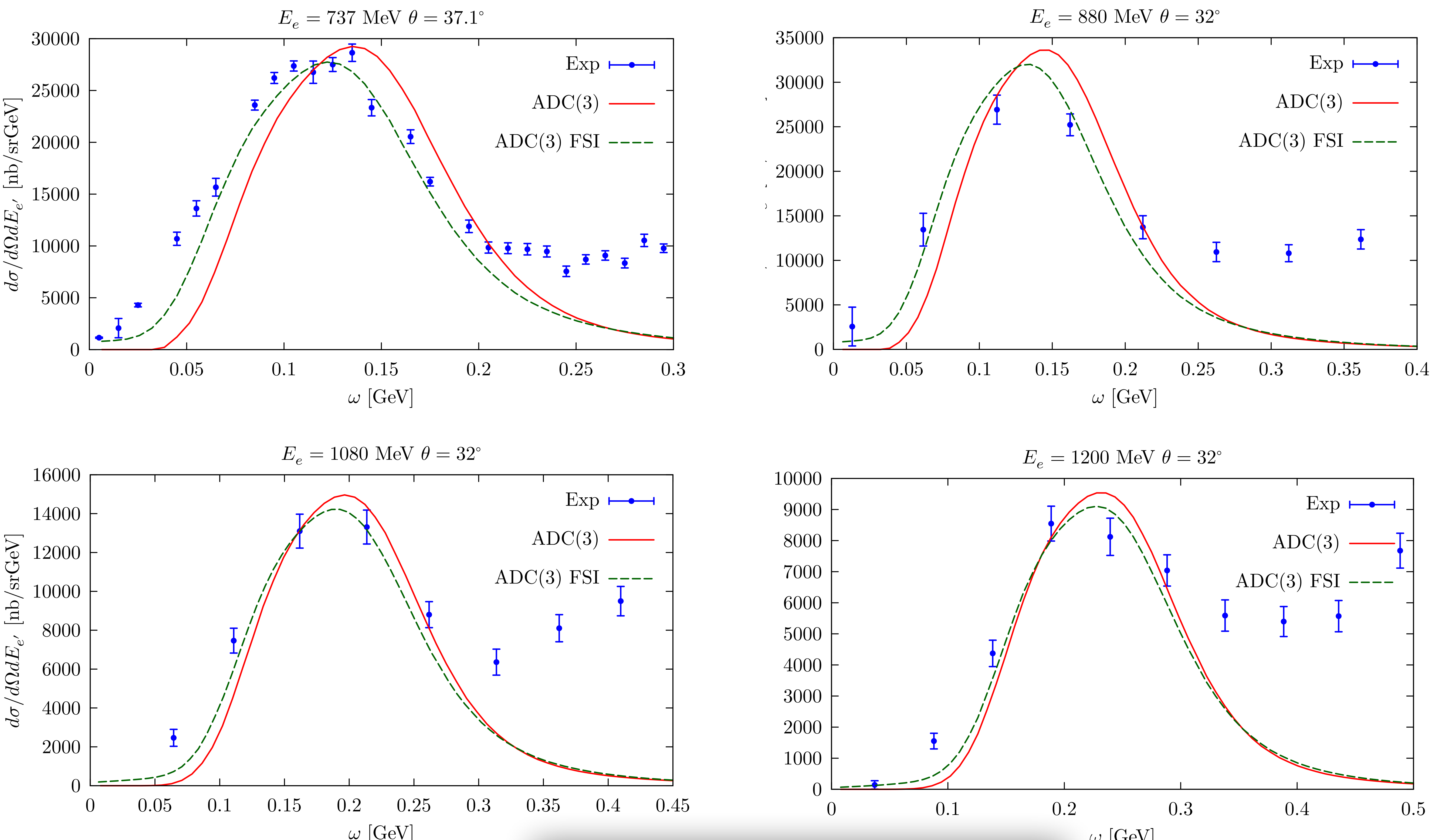

NR, C. Barbieri, Phys.Rev. C98 (2018) 025501

Preliminary results for ^{48}Ti(e,e') cross sections

C. Barbieri, NR, V. Somà, in Preparation

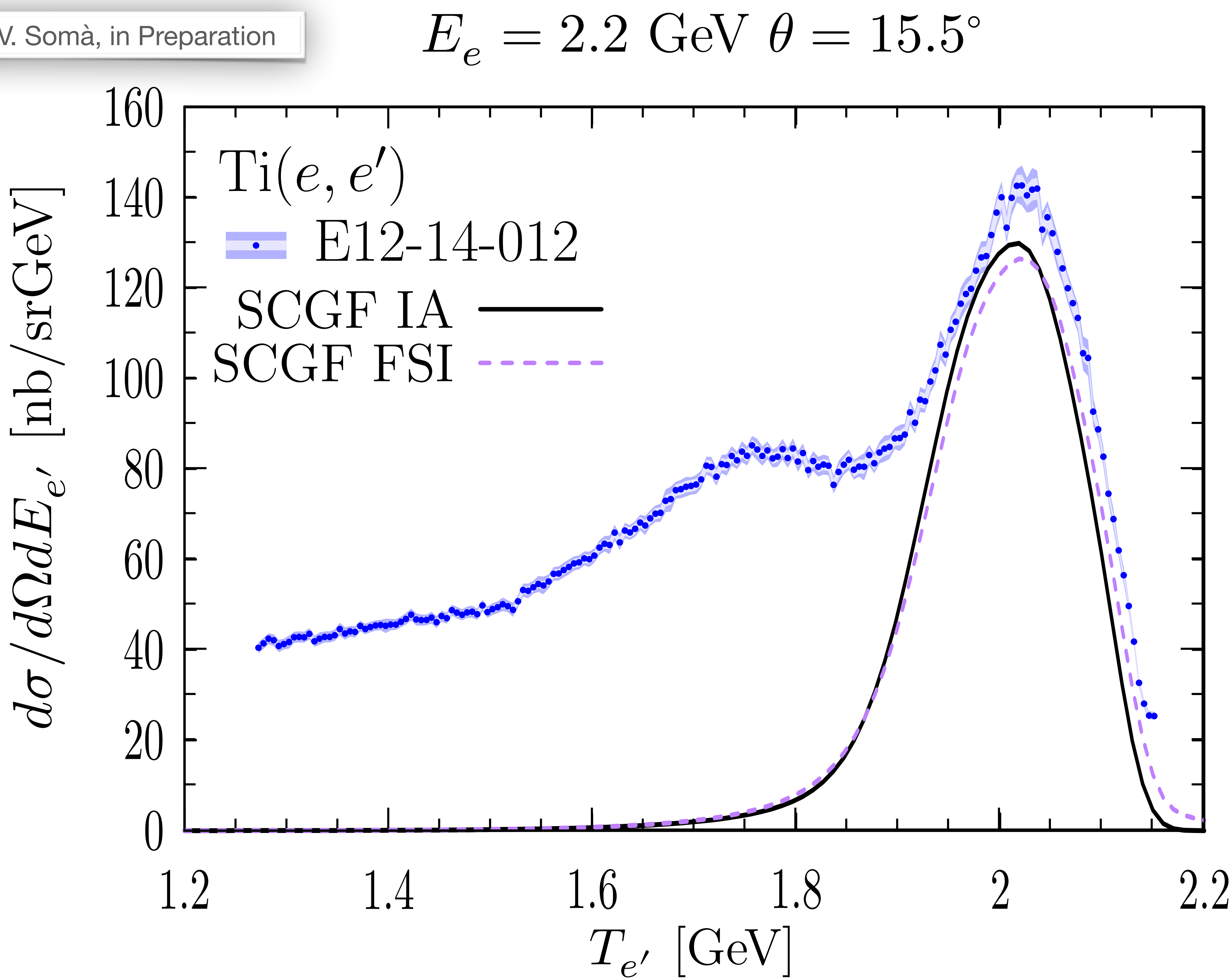

✤ Experimental data: Jefferson Lab Hall A Collaboration, Phys.Rev. C98 (2018) no.1, 014617

The CBF one-body Spectral Function of finite nuclei

- ^{12}C Spectral Function obtained within CBF and using the Local Density Approximation

$$P_{LDA}(\mathbf{k},E) = P_{MF}(\mathbf{k},E) + P_{corr}(\mathbf{k},E)$$

$$\int d^3r P^{NM}_{corr}(\mathbf{k},E;\rho=\rho_A(r))$$

$$\sum_n Z_n |\phi_n(\mathbf{k})|^2 F_n(E-E_n)$$

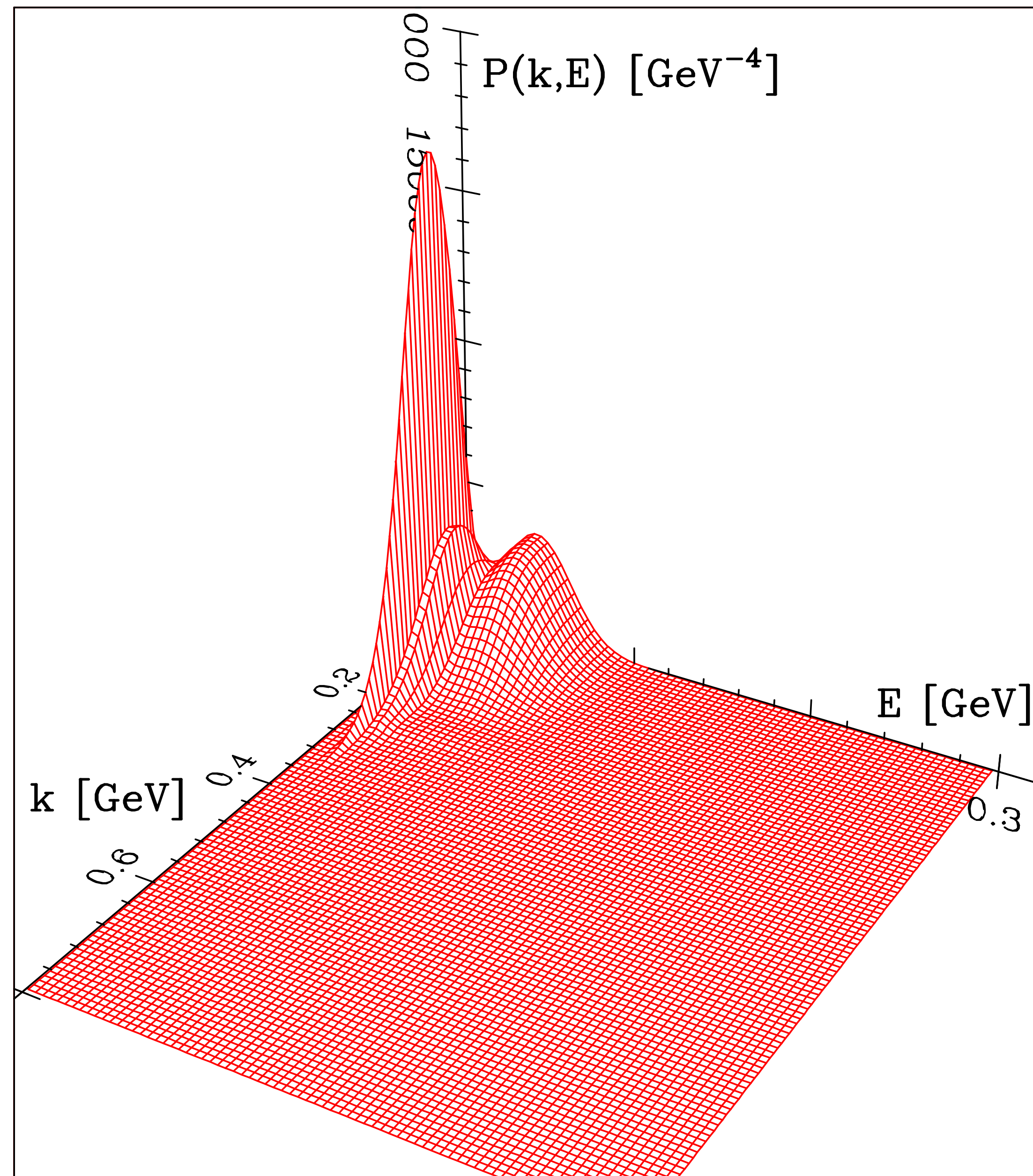

- Z_n : spectroscopic factor extracted from (e, e'p)
- F_n : finite width function accounting for residual interactions not included in a MF picture

- The one-body Spectral function of nuclear matter:

$$H = \sum_i \frac{\mathbf{p}_i^2}{2m} + \sum_{i<j} v_{ij} + \sum_{i<j<k} V_{ijk}$$

Argonne v18

UIX, IL7

O. Benhar, et al. RMP **80**, 189 (2008)

Production of two particle-two hole (2p2h) states

- Initial State Correlations

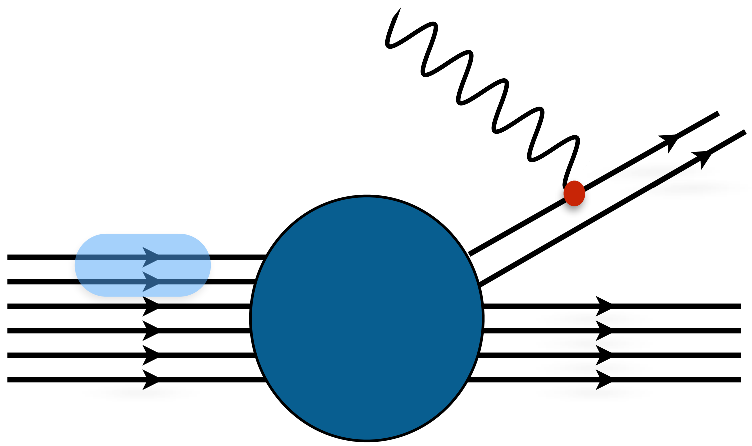

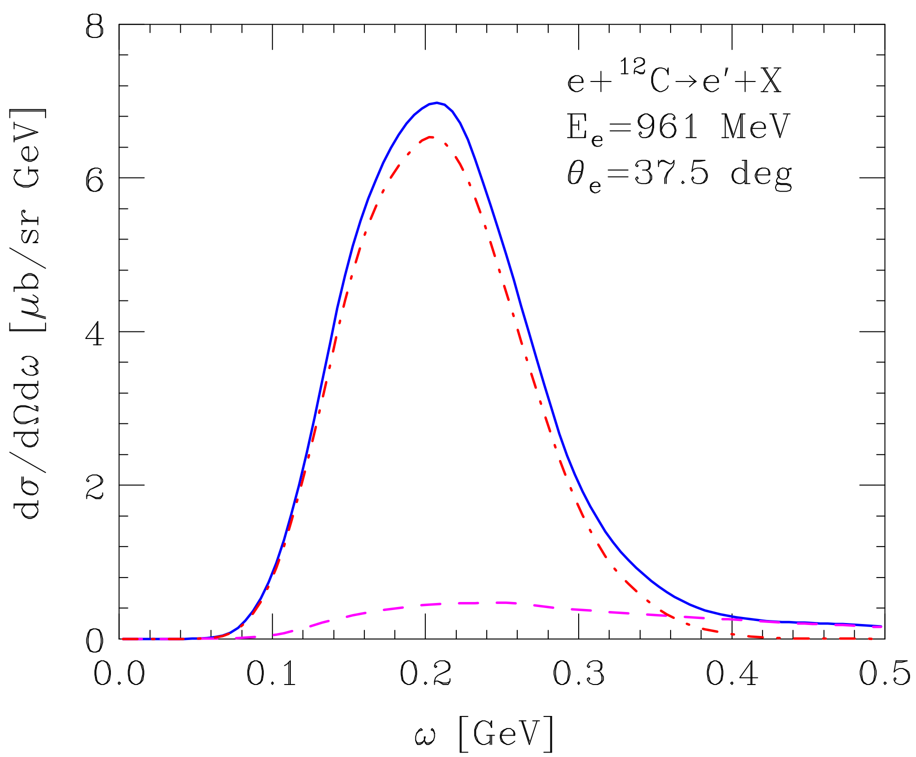

- $P_{corr}(\mathbf{k},E)$ accounts for the presence of strongly correlated pairs. Its contribution to the cross section is clearly visible: appearance of a tail in the large energy transfer region

- The Impulse Approximation is adopted

$$d\sigma_A = \int dE\, d^3k d\sigma_N P(\mathbf{k}, E)$$

O.Benhar, A.Lovato, NR, PRC92 (2015) , 024602

Production of two particle-two hole (2p2h) states

- Initial State Correlations

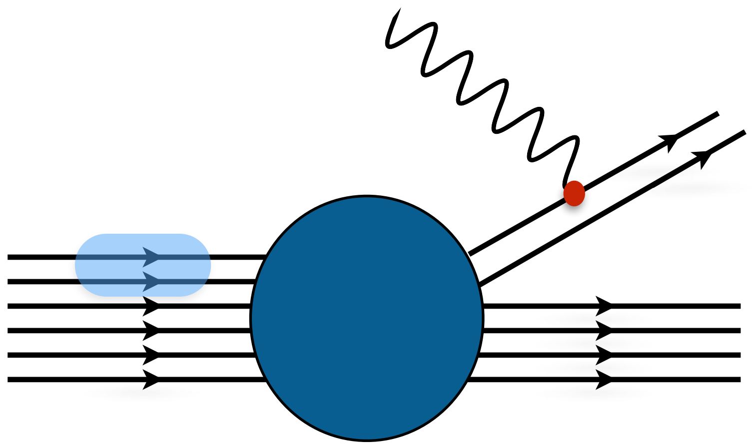

- Meson Exchange currents

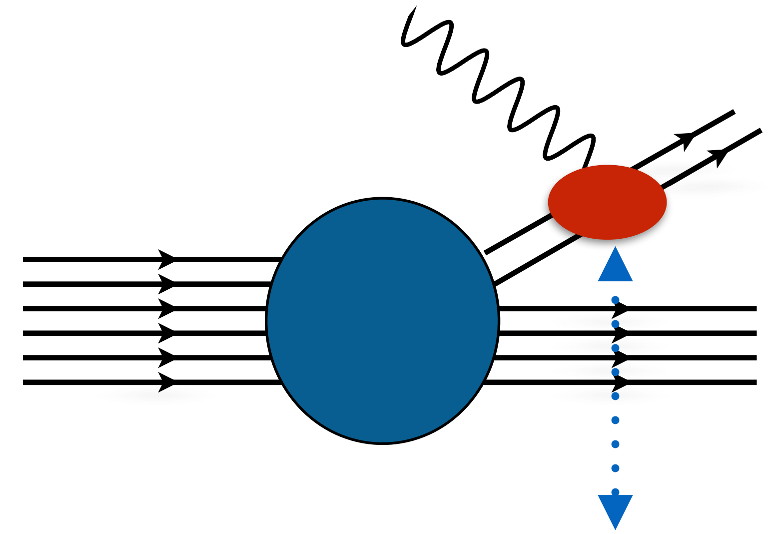

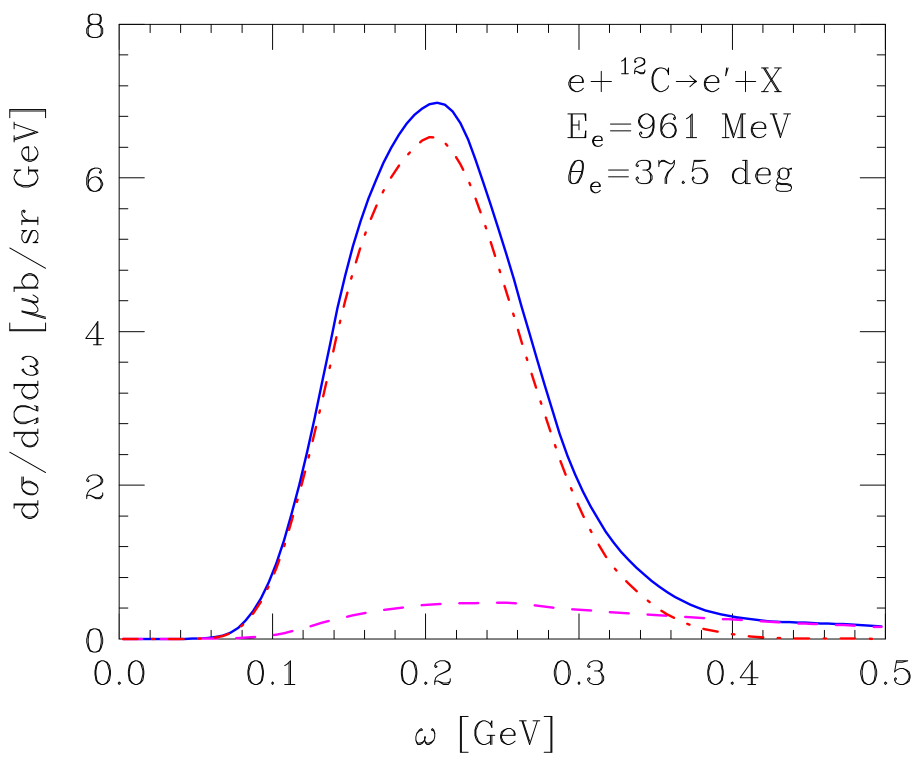

- $P_{corr}(\mathbf{k},E)$ accounts for the presence of strongly correlated pairs. Its contribution to the cross section is clearly visible: appearance of a tail in the large energy transfer region

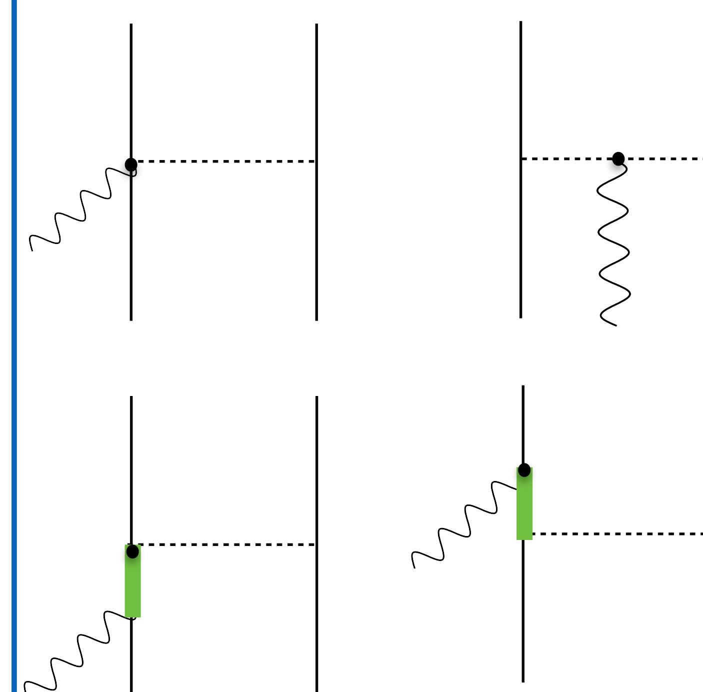

Different contributions to the relativistic two-body currents

O.Benhar, A.Lovato, NR, PRC92 (2015) , 024602

Production of two particle-two hole (2p2h) states

- Initial State Correlations

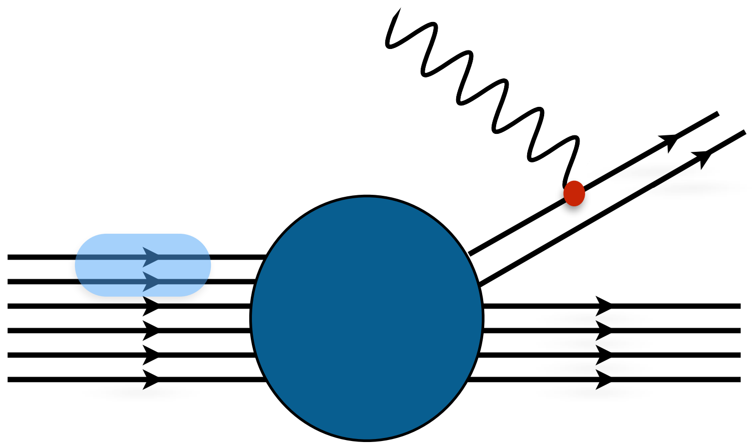

- Meson Exchange currents

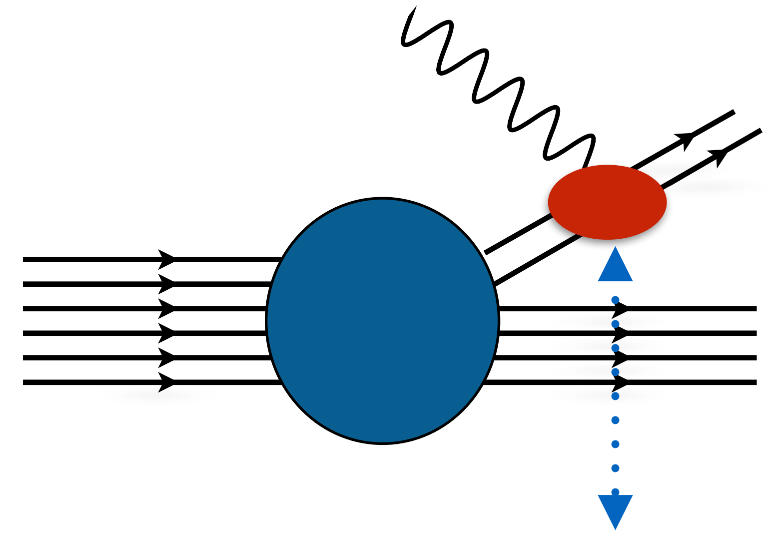

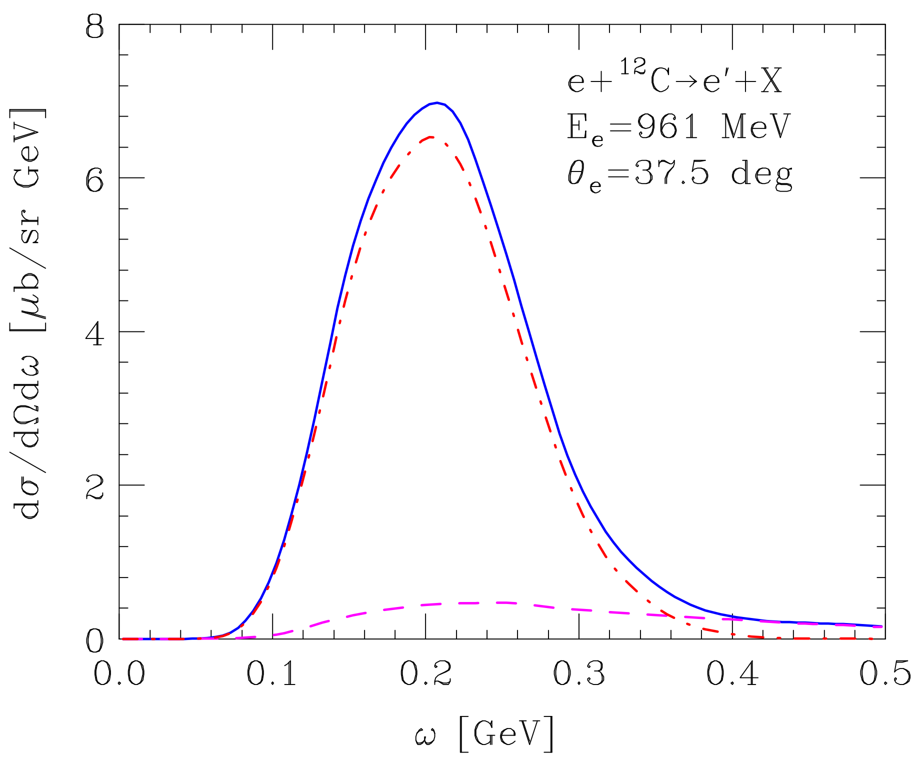

- $P_{corr}(\mathbf{k},E)$ accounts for the presence of strongly correlated pairs. Its contribution to the cross section is clearly visible: appearance of a tail in the large energy transfer region

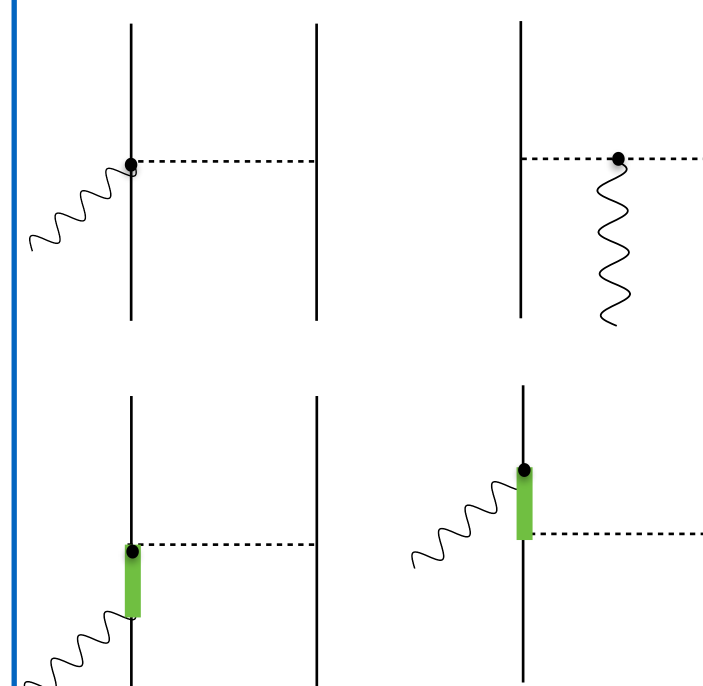

Different contributions to the relativistic two-body currents

- The Impulse Approximation has been generalized:

$$W^{\mu\nu}_{2p2h} = W^{\mu\nu}_{ISC} + W^{\mu\nu}_{MEC} + W^{\mu\nu}_{int}$$

O.Benhar, A.Lovato, NR, PRC92 (2015) , 024602

Results for $^{12}C(e,e')$ cross sections

- Separate contributions: IA

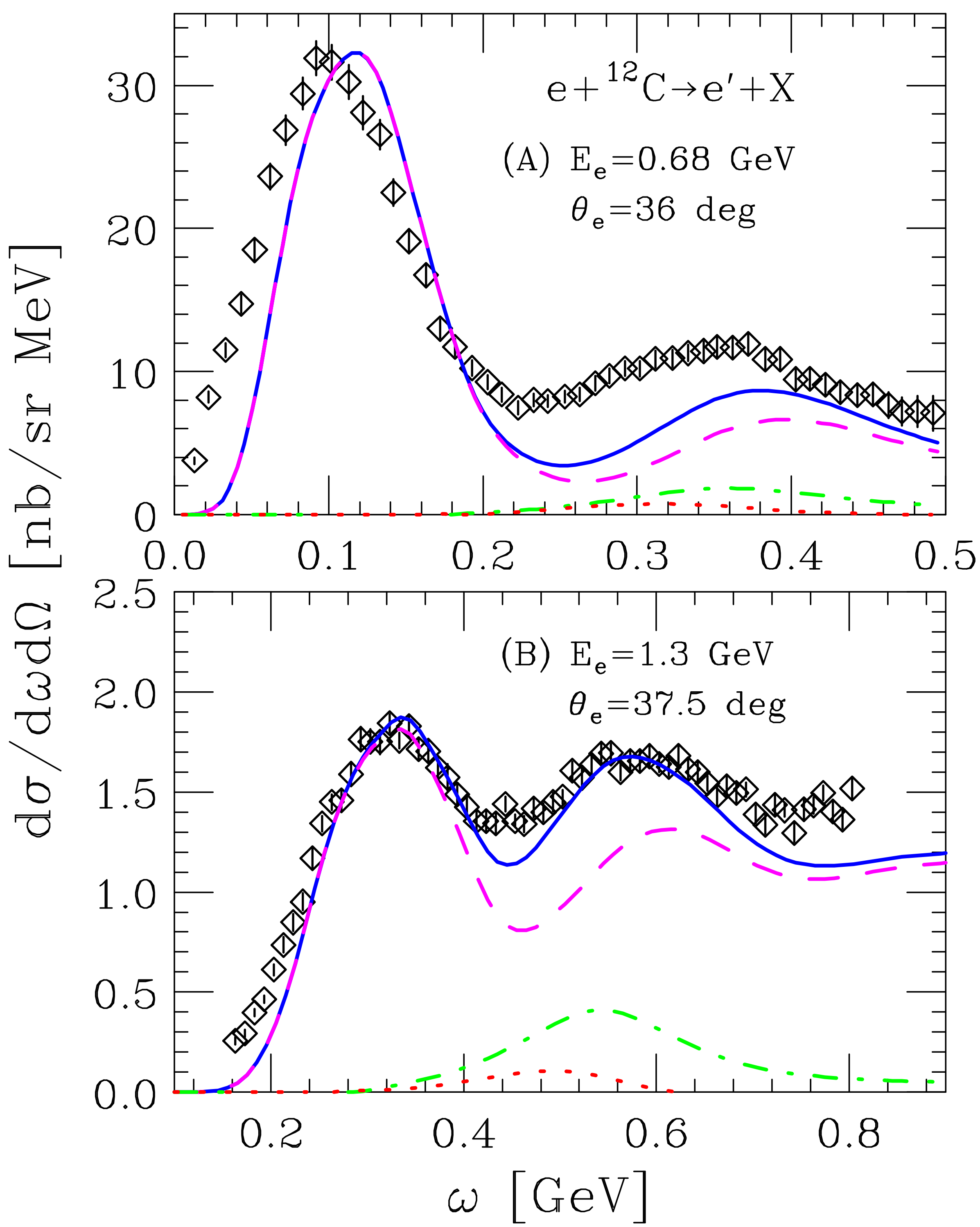

- Including FSI in the QE region

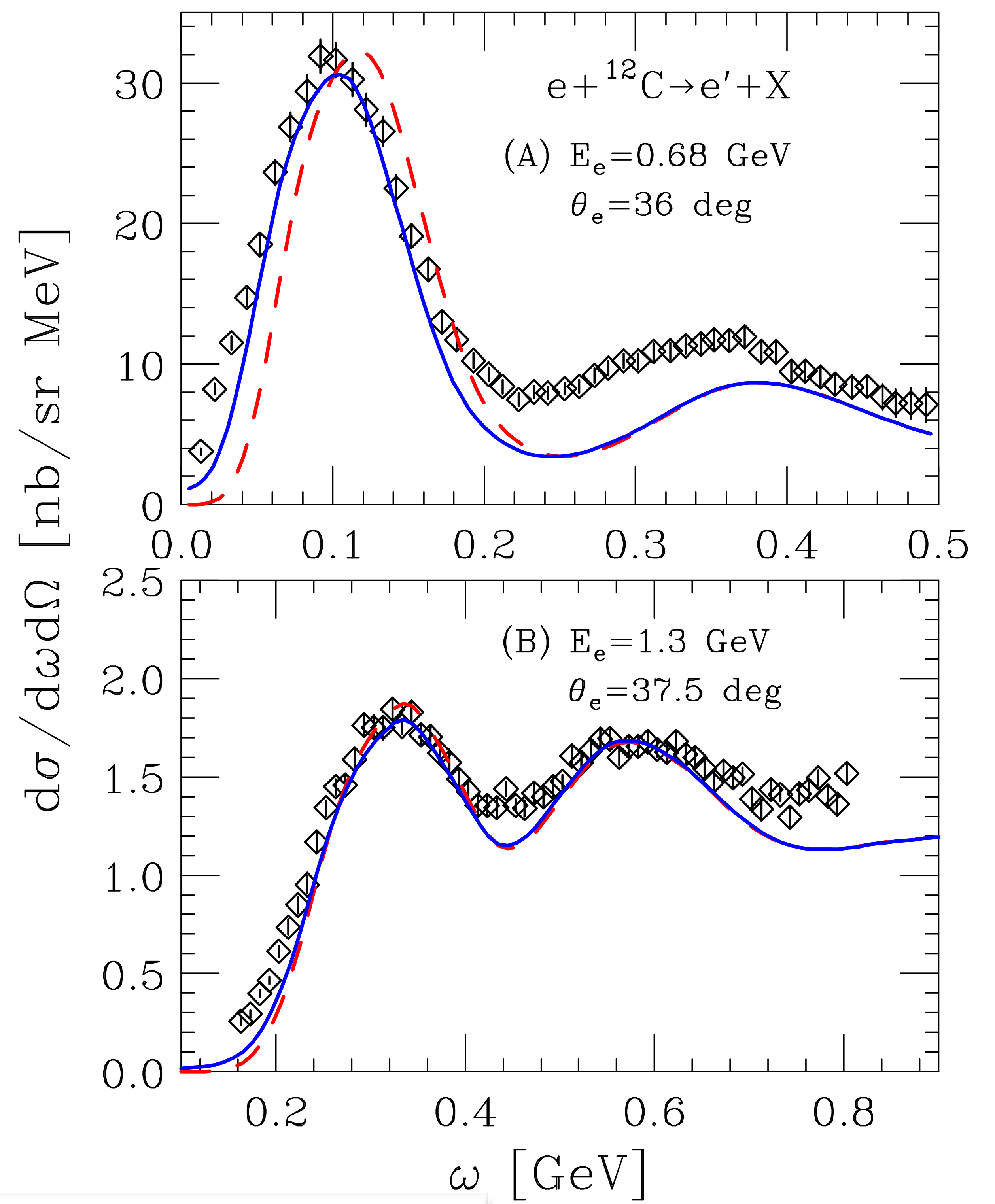

NR, A.Lovato, O.Benhar, PRL 116, 192501 (2016)

(Anti)neutrino -^{12}C scattering cross sections

The inclusive cross section of the process in which a neutrino or antineutrino scatters off a nucleus can be written in terms of five response functions

$$\frac{d\sigma}{dE_{\ell'}d\Omega_\ell} \propto [v_{00}R_{00} + v_{zz}R_{zz} - v_{0z}R_{0z} + v_{xx}R_{xx} \mp v_{xy}R_{xy}]$$

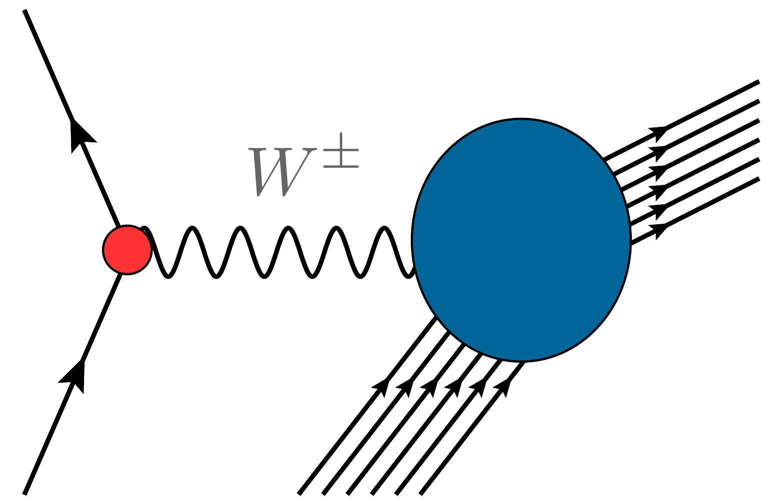

- We generalized the SF formalism to include vector and axial vector relativistic two-body currents

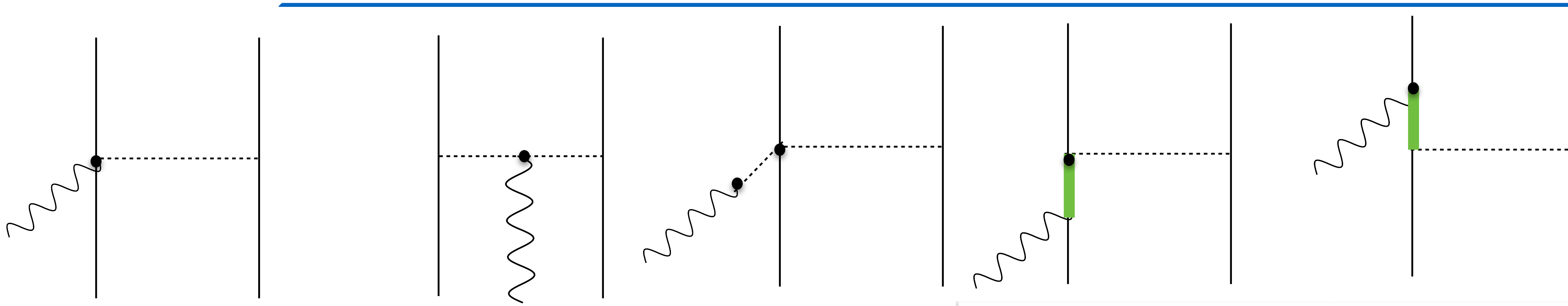

E. Hernandez et al. PRD 76, 033005 (2007)

- The calculation of the MEC current matrix is carried out automatically
- 9d-integral + use of realistic SFs implies dealing with a broader phase space (see W. Van Orden's talk) : we developed an highly parallel Monte Carlo code, importance sampling procedure

Two-body CC response functions of ^{12}C

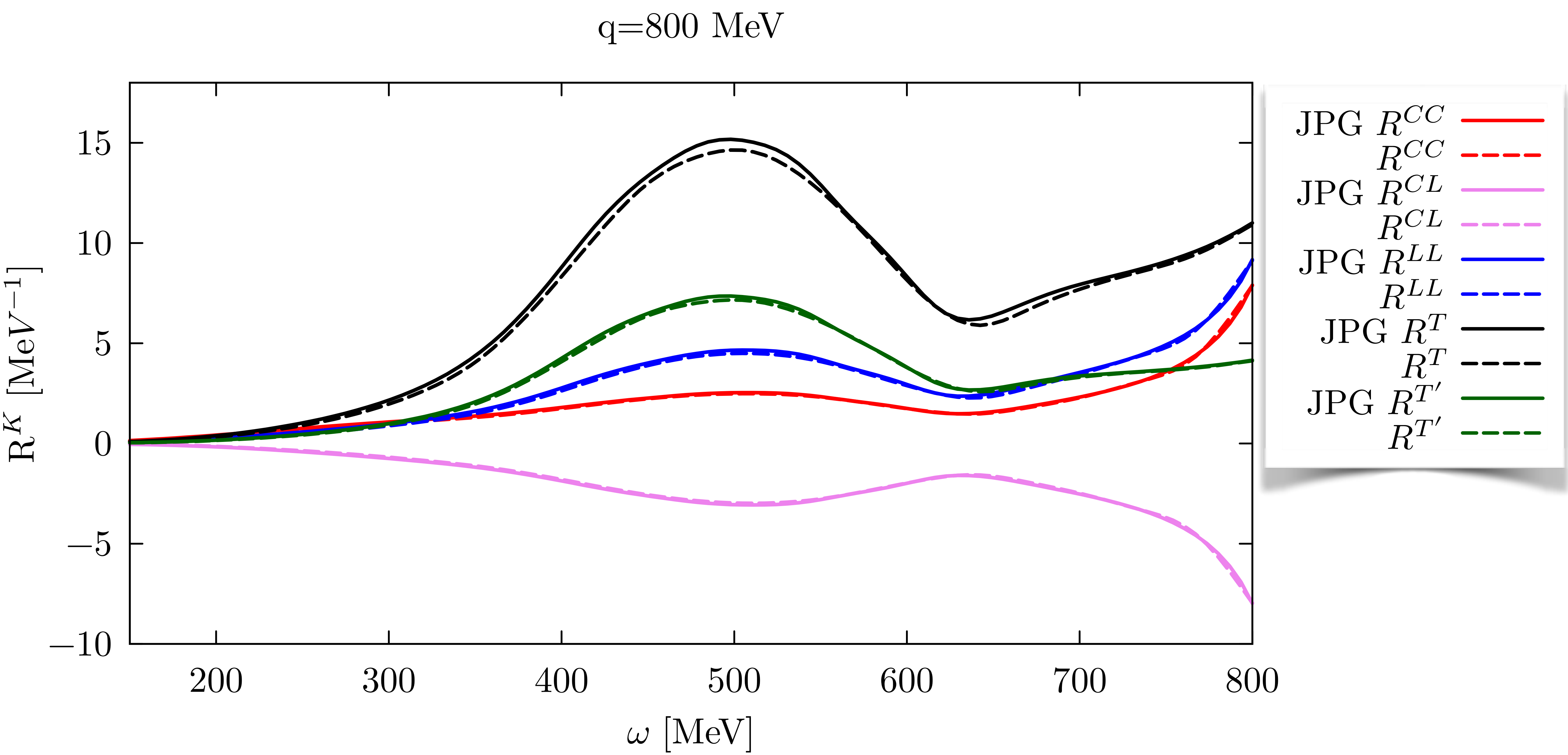

- Comparison of the five CC response functions of ^{12}C with the results of I. Ruiz Simo, et. al, Journal of Phys. G 44, no. 6 (2017).

- In this case, we approximated the two-body spectral function with that of the global relativistic Fermi gas model

CCQE neutrino -^{12}C cross sections

NR, C.Barbieri, O. Benhar, A. Lovato, in Preparation

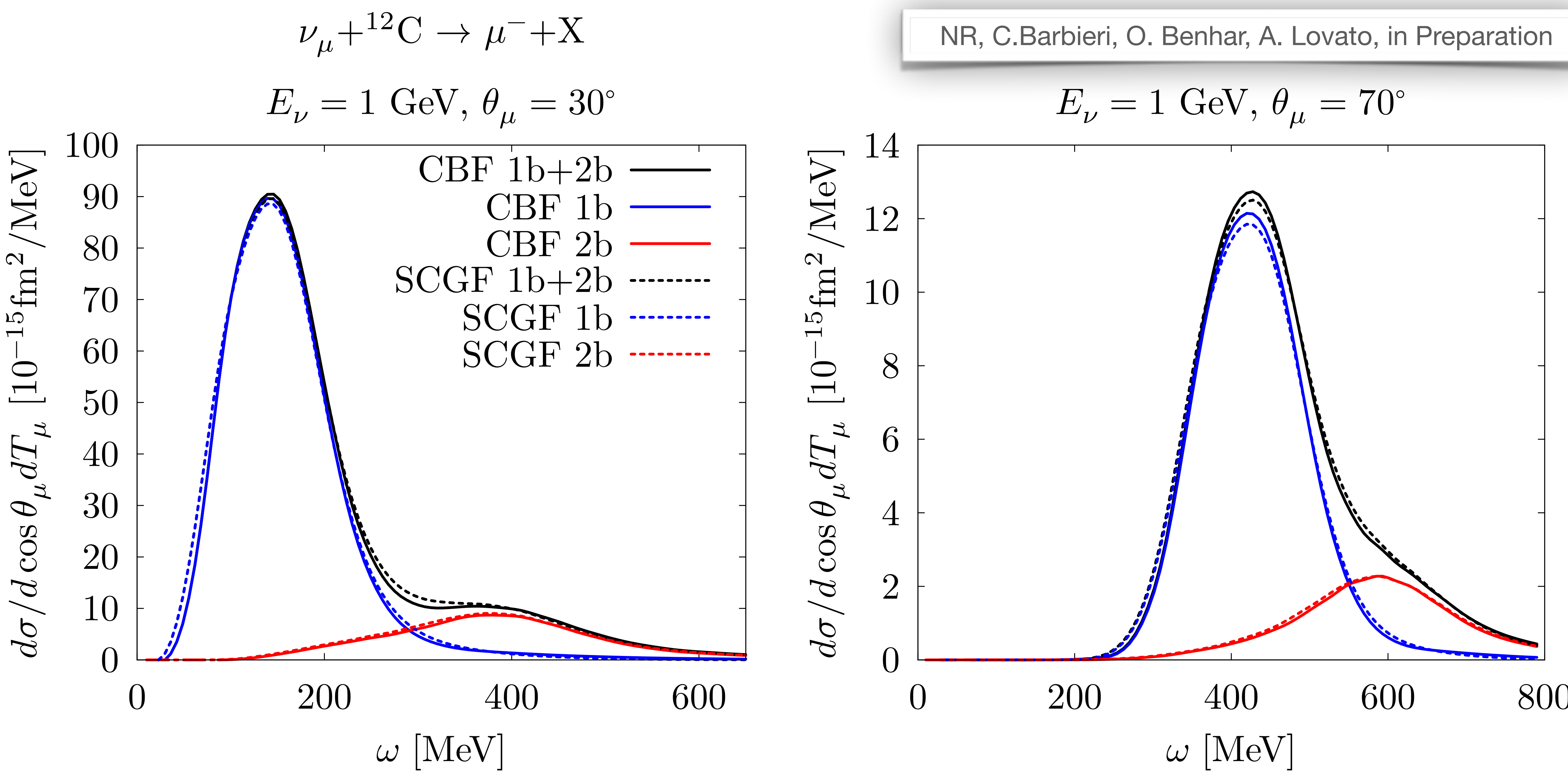

- The 2b contribution mostly affects the 'dip' region, in analogy with the electromagnetic case
- Meson exchange currents strongly enhance the cross section for large values of the scattering angle

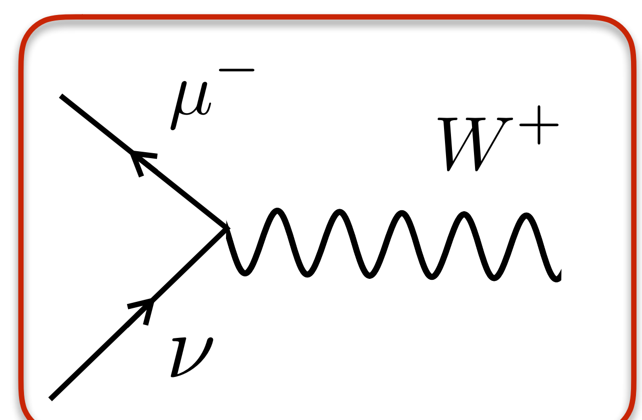

CCQE antineutrino -^{12}C cross sections

NR, C.Barbieri, O. Benhar, A. Lovato, in Preparation

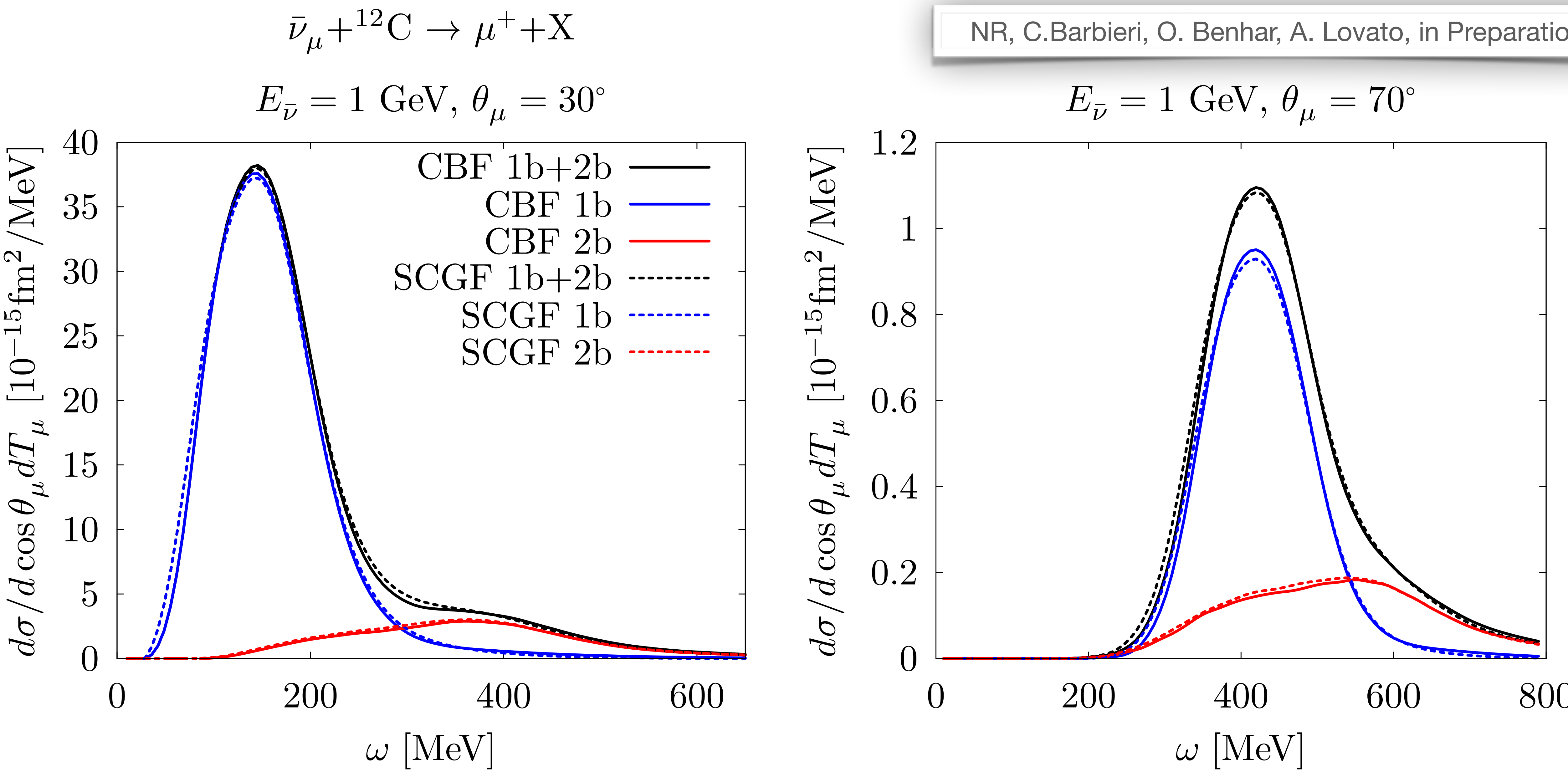

- The 2b contribution mostly affects the 'dip' region, in analogy with the electromagnetic case
- Meson exchange currents strongly enhance the cross section for large values of the scattering angle

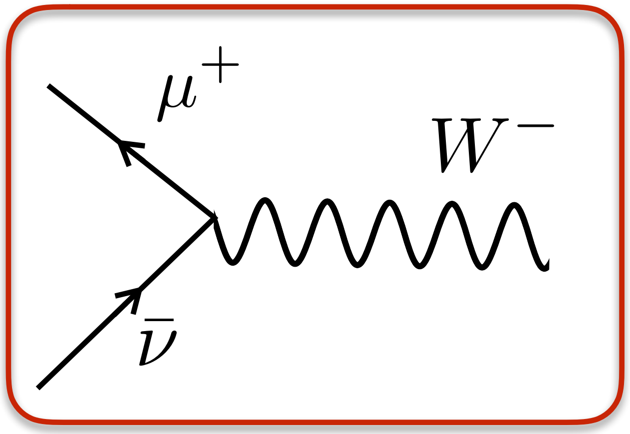

NCQE neutrino -^{12}C cross sections

NR, C.Barbieri, O. Benhar, A. Lovato, in Preparation

$$\nu_\mu + {}^{12}\mathrm{C} \rightarrow \nu_\mu + \mathrm{X}$$

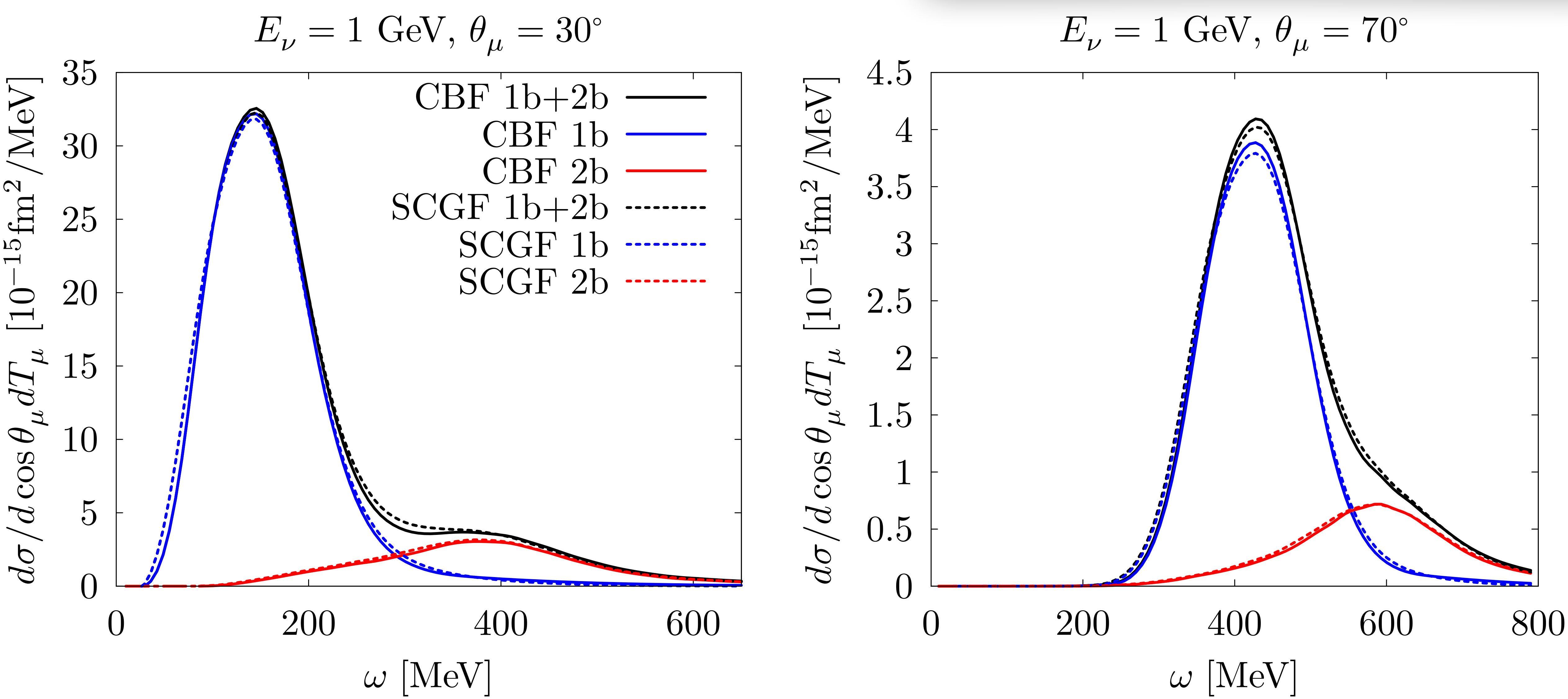

- The 2b contribution mostly affects the 'dip' region, in analogy with the electromagnetic case

- Meson exchange currents strongly enhance the cross section for large values of the scattering angle

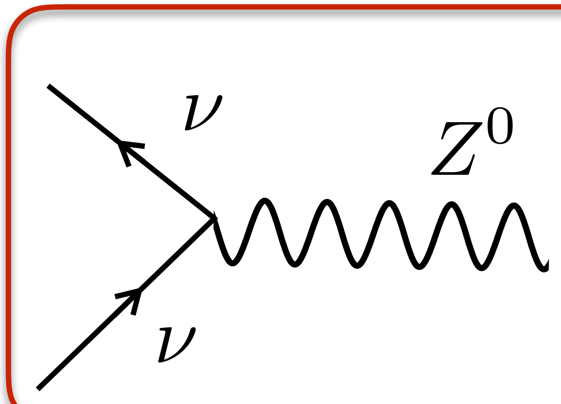

NCQE antineutrino -^{12}C cross sections

NR, C.Barbieri, O. Benhar, A. Lovato, in Preparation

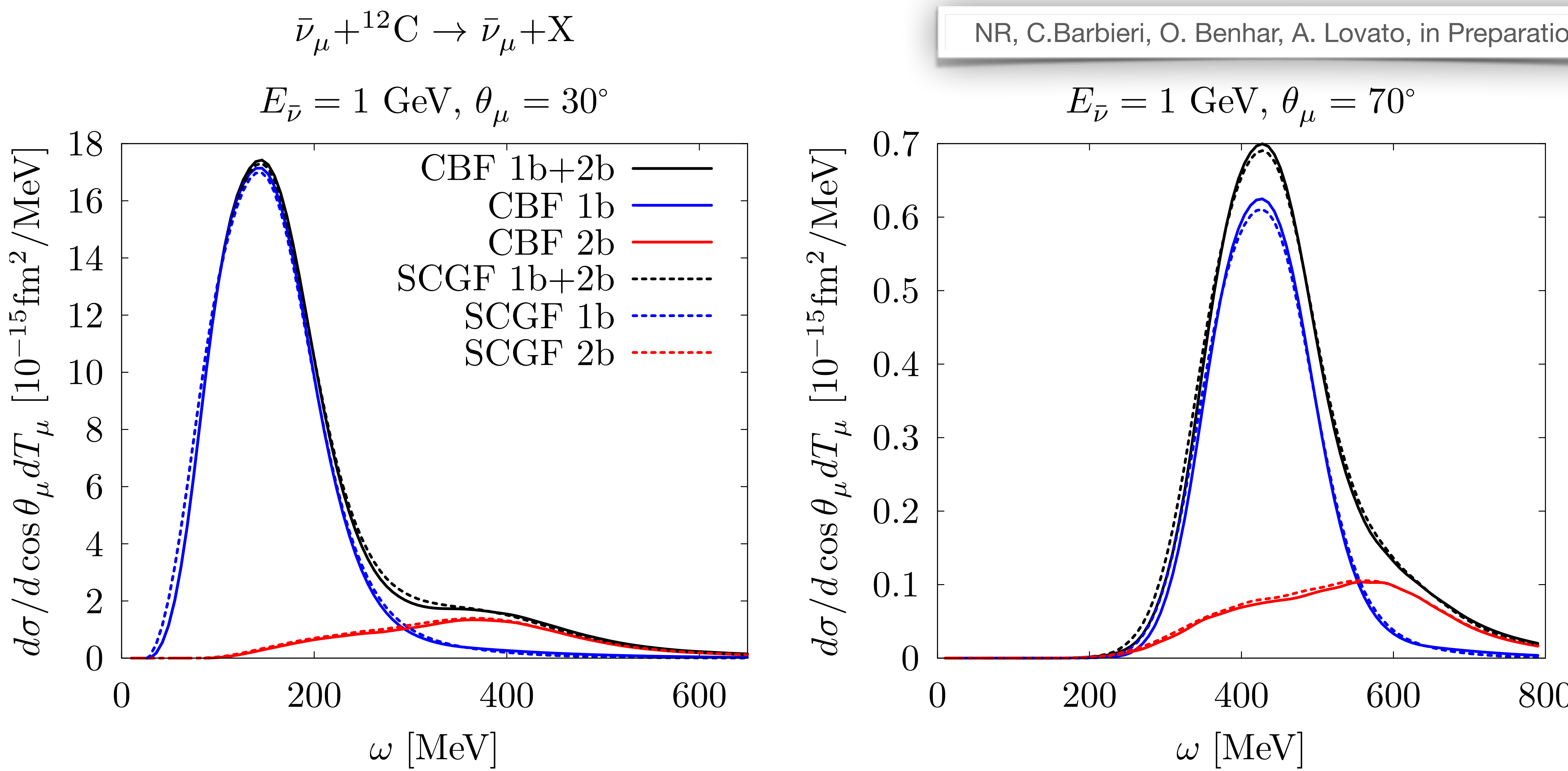

- The 2b contribution mostly affects the 'dip' region, in analogy with the electromagnetic case

- Meson exchange currents strongly enhance the cross section for large values of the scattering angle

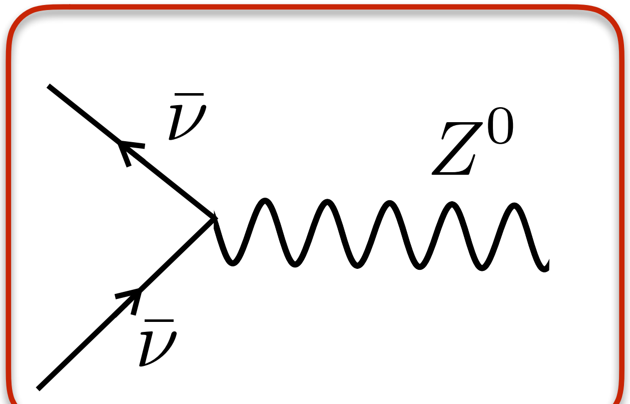

CCQE neutrino -^{12}C total cross section

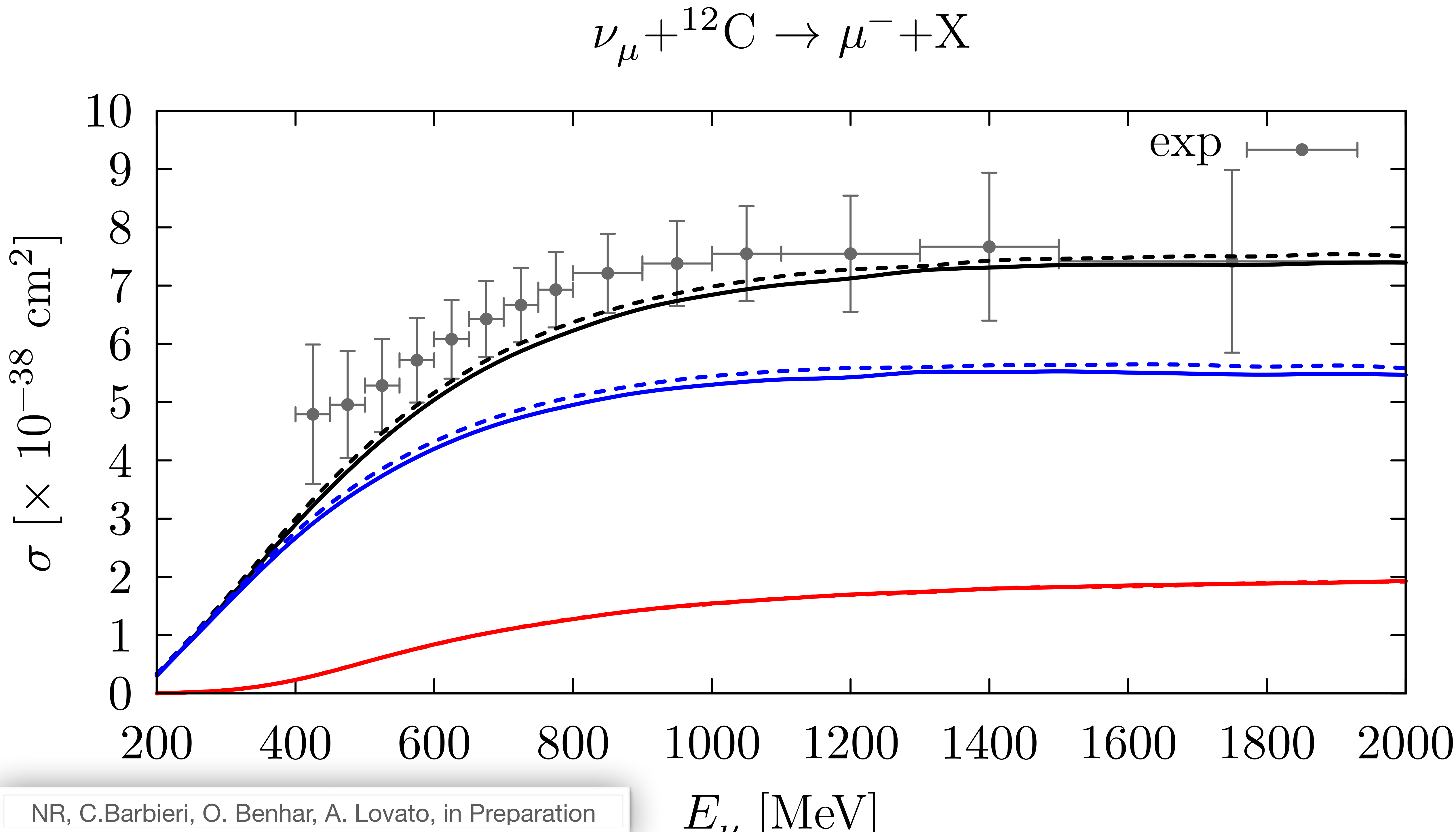

NR, C.Barbieri, O. Benhar, A. Lovato, in Preparation

- The 2p2h contribution is needed to explain the size of the measured cross section

CCQE antineutrino -^{12}C total cross section

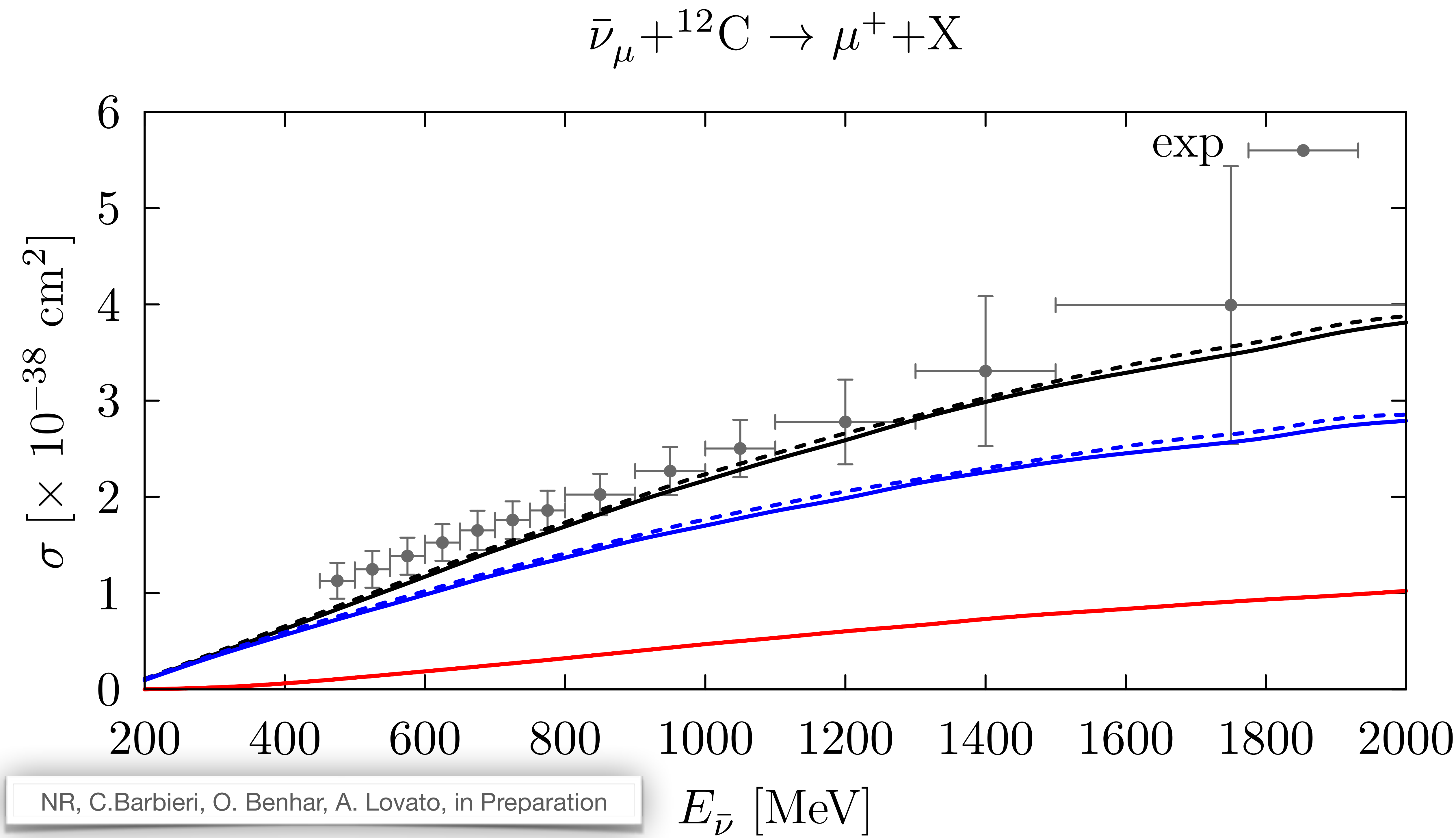

NR, C.Barbieri, O. Benhar, A. Lovato, in Preparation

- The 2p2h contribution is needed to explain the size of the measured cross section

Prospects

- Correlated Basis Function and Self Consistent Green's Function approach :
  - ❖ Flux-folded double differential inclusive cross sections for CC0π and NC0π processes
  - ❖ Inclusion of the interference between one- and two-body currents: benchmark with GFMC
- Self Consistent Green's Function approach :
  - ❖ CCQE - NCQE Ti^{48} and Ar^{40} neutrino and antineutrino cross section
  - ❖ Investigating the difference between the structure of the Ti^{48} proton and Ar^{40} neutron spectral function
- Green's Function Monte Carlo approach :
  - ❖ Spectral Function calculation of light nuclei within GFMC with both phenomenological and chiral Hamiltonians
  - ❖ The use of different potentials can provide an estimate of the theoretical uncertainty of the calculation

Back up slides

Relativistic effects in a correlated system

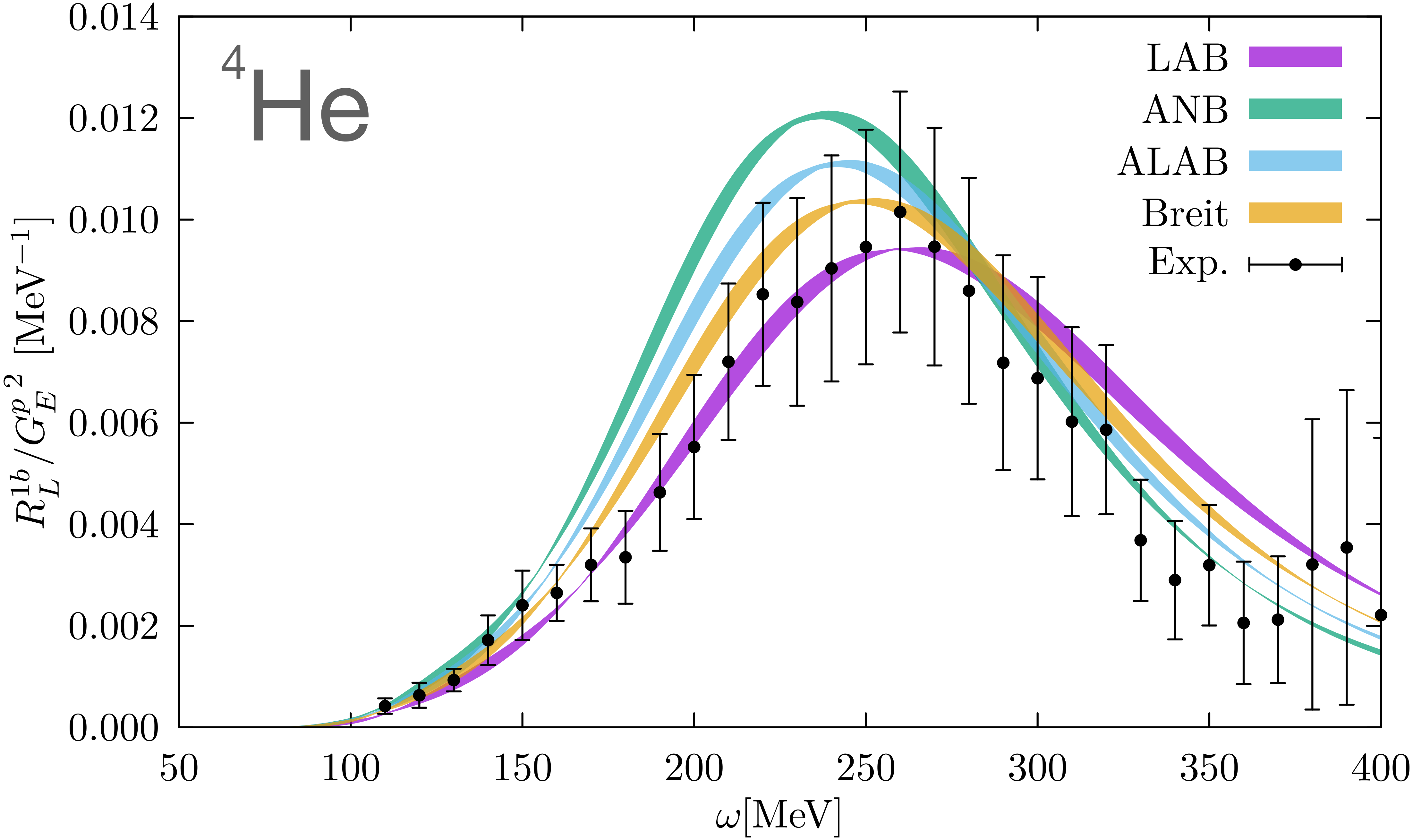

- Longitudinal responses of ^{4}He for |q|=700 MeV in the four different reference frames. The curves show differences in both peak positions and heights.

Relativistic effects in a correlated system

- The frame dependence can be drastically reduced if one assumes a two-body breakup model with relativistic kinematics to determine the input to the non relativistic dynamics calculation

$$p^{fr} = \mu\Big(\frac{p_N^{fr}}{m_N} - \frac{p_X^{fr}}{M_X}\Big) \quad \longleftrightarrow \quad \mu = \frac{m_N M_X}{m_N + M_X}$$

$$P_f^{fr} = p_N^{fr} + p_X^{fr}$$

- The relative momentum is derived in a relativistic fashion

$$\omega^{fr} = E_f^{fr} - E_i^{fr}$$

$$E_f^{fr} = \sqrt{m_N^2 + [\mathbf{p}^{fr} + \mu/M_X \mathbf{P}_f^{fr}]^2} + \sqrt{M_X^2 + [\mathbf{p}^{fr} - \mu/m_N \mathbf{P}_f^{fr}]^2}$$

- And it is used as input in the non relativistic kinetic energy

$$e_f^{fr} = (p^{fr})^2/(2\mu)$$

- The energy-conserving delta function reads

$$\delta(E_f^{fr} - E_i^{fr} - \omega^{fr}) = \delta(F(e_f^{fr}) - \omega^{fr}) = \Big(\frac{\partial F^{fr}}{\partial e_f^{fr}}\Big)^{-1} \delta[e_f^{fr} - e_f^{rel}(q^{fr}, \omega^f)]$$

Relativistic effects in a correlated system

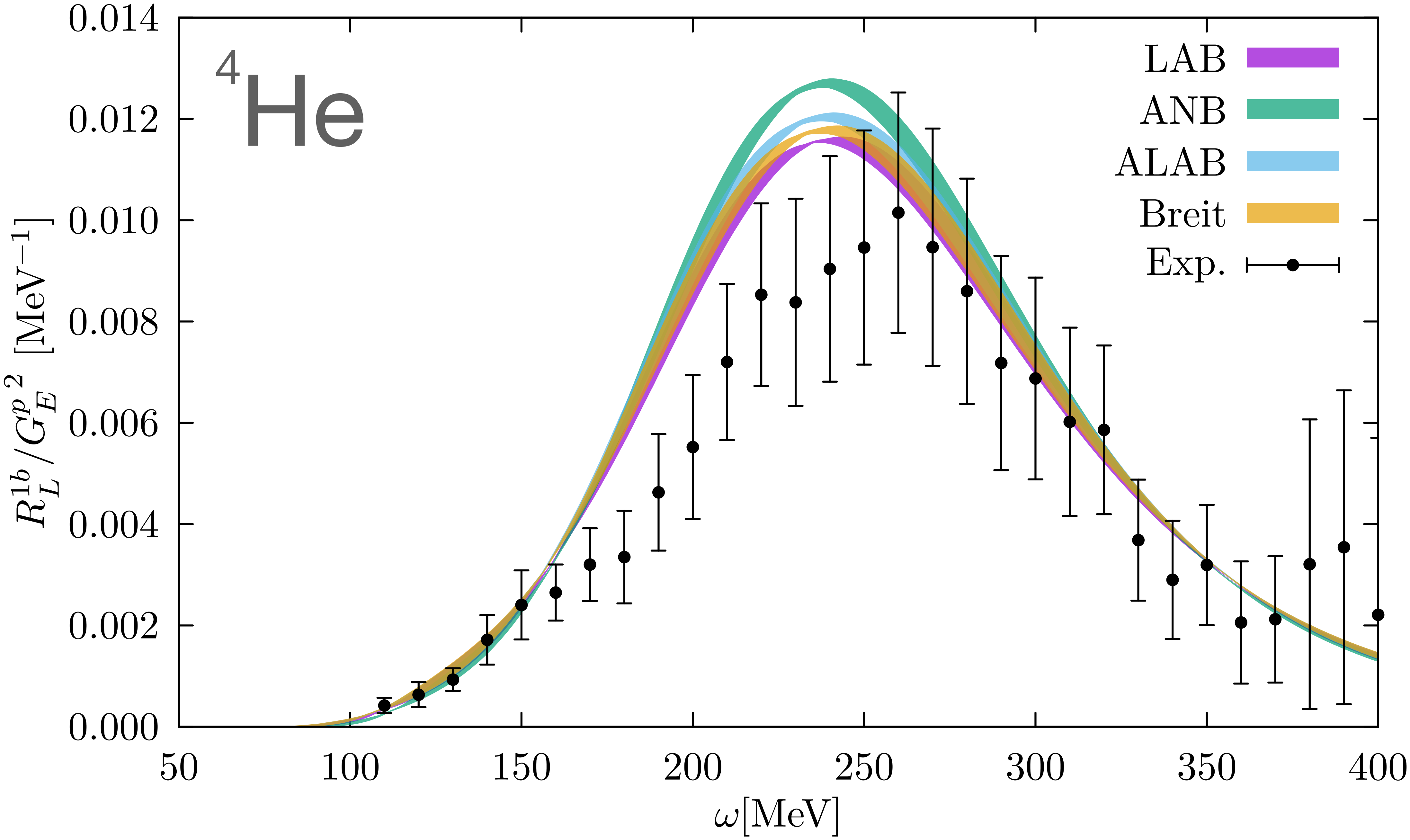

- Longitudinal responses of ^{4}He for |q|=700 MeV in the four different reference frames. The different curves are almost identical.

Extension of the factorization scheme to two-nucleon emission amplitude

$$|X\rangle \longrightarrow |\mathbf{p}\ \mathbf{p}'\rangle \otimes |n_{(A-2)}\rangle = |n_{(A-2)};\mathbf{p}\ \mathbf{p}'\rangle \ ,$$

We can introduce the two-nucleon Spectral Function. . .

$$P(\mathbf{k},\mathbf{k}',E) = \sum_n |\langle n_{(A-2)};\mathbf{k}\ \mathbf{k}'|0\rangle|^2 \delta(E + E_0 - E_n)$$

probability of removing two nucleons leaving the A-2 system with energy E

The pure 2-body & the interference contribution to the hadron tensor read

$$W^{\mu\nu}_{2p2h,22} \propto \int d^3k d^3k' d^3p d^3p' \int dE\ P_{2h}(\mathbf{k},\mathbf{k}',E)\langle \mathbf{k}\mathbf{k}'|j^{\mu}_{12}|\mathbf{p}\mathbf{p}'\rangle\langle \mathbf{p}\mathbf{p}'|j^{\nu}_{12}|\mathbf{k}\mathbf{k}'\rangle$$

$$W^{\mu\nu}{}_{2p2h,12} \propto \int d^3k\ d^3\xi\ d^3\xi'\ d^3h\ d^3h' d^3p\ d^3p' \phi^{hh'\,*}_{\xi\xi'} \langle \mathbf{p},\mathbf{p}'|j^{\nu}_{12}|\boldsymbol{\xi},\boldsymbol{\xi}'\rangle \left[\Phi^{hh'p'}_{k}\langle \mathbf{k}|j^{\mu}_{1}|\mathbf{p}\rangle + \Phi^{hh'p}_{k}\langle \mathbf{k}|j^{\mu}_{2}|\mathbf{p}'\rangle\right]$$

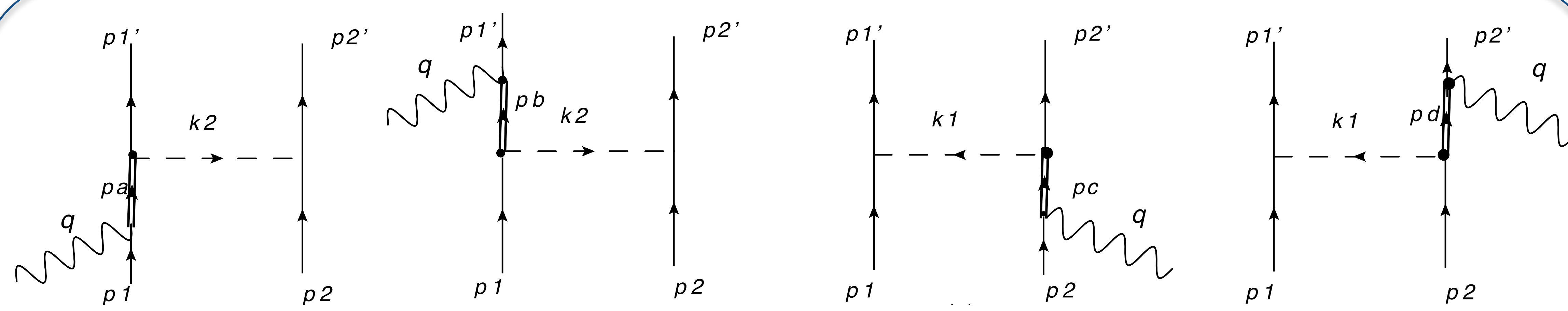

The Rarita-Schwinger (RS) expression for the Δ propagator reads

$$S^{\beta\gamma}(p, M_\Delta) = \frac{\not{p} + M_\Delta}{p^2 - M_\Delta^2}\left(g^{\beta\gamma} - \frac{\gamma^\beta\gamma^\gamma}{3} - \frac{2p^\beta p^\gamma}{3M_\Delta^2} - \frac{\gamma^\beta p^\gamma - \gamma^\gamma p^\beta}{3M_\Delta}\right)$$

WARNING

If the condition $p_\Delta^2 > (m_N + m_\pi)^2$ the real resonance mass has to be replaced by $M_\Delta \longrightarrow M_\Delta - i\Gamma(s)/2$ where $\Gamma(s) = \frac{(4f_{\pi N\Delta})^2}{12\pi m_\pi^2}\frac{k^3}{\sqrt{s}}(m_N + E_k)$.

Hadronic monopole form factors

$$F_{\pi NN}(k^2) = \frac{\Lambda_\pi^2 - m_\pi^2}{\Lambda_\pi^2 - k^2}$$

$$F_{\pi N\Delta}(k^2) = \frac{\Lambda_{\pi N\Delta}^2}{\Lambda_{\pi N\Delta}^2 - k^2}$$

and the EM ones

$$F_{\gamma NN}(q^2) = \frac{1}{(1 - q^2/\Lambda_D^2)^2} \ ,$$

$$F_{\gamma N\Delta}(q^2) = F_{\gamma NN}(q^2)\Big(1 - \frac{q^2}{\Lambda_2^2}\Big)^{-1/2}\Big(1 - \frac{q^2}{\Lambda_3^2}\Big)^{-1/2}$$

where $\Lambda_\pi = 1300$ MeV, $\Lambda_{\pi N\Delta} = 1150$ MeV, $\Lambda_D^2 = 0.71\mathrm{GeV}^2$, $\Lambda_2 = M + M_\Delta$ and $\Lambda_3^2 = 3.5\ \mathrm{GeV}^2$.